Chemistry–A European Journal

Supporting Information

Quantitative Structure-Property Relationship Modelling for the Prediction of Singlet Oxygen Generation by Heavy-Atom-Free BODIPY Photosensitizers**

Andrey A. Buglak, Asterios Charisiadis, Aimee Sheehan, Christopher J. Kingsbury, Mathias O. Senge,* and Mikhail A. Filatov*

Supplementary Information

Contents

1. BODIPY dataset S2

2. Synthetic Procedures and Characterization S11

2.1 Materials and Instruments S12

2.2 Chemical Synthesis of BDP 1-7 ..... S12

2.3 NMR and HRMS Data S14

2.4 Crystallographic Data S24

2.5 Optical Spectra S25

3. Computational methods and results S28

4. Singlet oxygen generation quantum yields measurements S31

5. Supplemental Crystal Structure Images S40

6. References S43

1. BODIPY dataset

Table S1. The structures and singlet oxygen quantum yield values (Φ_Δ) of heavy-atom-free BODIPYs dyes in different solvents, as searched from chemical databases. Φ_Δ values used in Models 1-3 are highlighted.

Structure	Solvent	Φ_Δ	Comment[a,b,c]	Reference
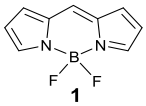 1	hexane	0.066	A = DPIBF; S = MeSBDPI$_2$; λ_{exc} = 509 nm; [O_2] = air	1
	toluene	0.12		1
	THF	0.071		1
	MeOH	0.083		1
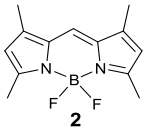 2	hexane	0.03	A = DPIBF; S = MeSBDPI$_2$; λ_{exc} = 540 nm; [O_2] = air	2
	toluene	0.061		2
	CCl_4	0.100		2
	CH_2Cl_2	0.062		2
	THF	0.091		2
	EtOH	0.058		2
	CH_3CN	0.069		2
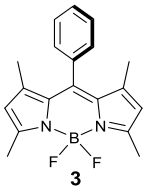 3	hexane	0.038	A = DPIBF; S = MeSBDPI$_2$; λ_{exc} = 509 nm; [O_2] = air	3
	toluene	0.023	A = DPIBF; S = MeSBDPI$_2$; λ_{exc} = 540 nm; [O_2] = air	4
	EtOAc	0.052	A = DPIBF; S = MeSBDPI$_2$; λ_{exc} = 509 nm; [O_2] = air	3
	THF	0.13	A = DPIBF; S = MeSBDPI$_2$; λ_{exc} = 540 nm; [O_2] = air	4
	pinacolone	0.11	A = DPIBF; S = MeSBDPI$_2$; λ_{exc} = 509 nm; [O_2] = air	3
	acetone	0.050		3
	EtOH	0.030	A = DPIBF; S = MeSBDPI$_2$; λ_{exc} = 540 nm; [O_2] = air	4
	MeOH	0.031	A = DPIBF; S = MeSBDPI$_2$; λ_{exc} = 509 nm; [O_2] = air	3
	CH_3CN	0.017	A = DPIBF; S = MeSBDPI$_2$; λ_{exc} = 540 nm; [O_2] = air	4
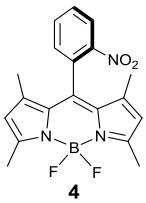 4	hexane	0.018	A = DPIBF; S = MeSBDPI$_2$; λ_{exc} = 509 nm; [O_2] = air	3
	EtOAc	0.027		3
	THF	0.026		3
	pinacolone	0.079		3
	acetone	0.051		3
	MeOH	0.0083		3
	CH_3CN	0.020		3
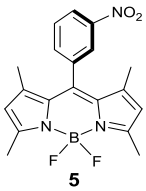 5	hexane	0.01	A = DPIBF; S = MeSBDPI$_2$; λ_{exc} = 509 nm; [O_2] = air	3
	EtOAc	0.031		3
	THF	0.028		3
	pinacolone	0.07		3
	acetone	0.029		3
	MeOH	0.0062		3
	CH_3CN	0.0044		3
	hexane	0.0067	A = DPIBF; S = MeSBDPI$_2$; λ_{exc} = 509 nm; [O_2] = air	3
	EtOAc	0.021		3
	THF	0.019		3
	pinacolone	0.047		3
	acetone	0.0093		3
	MeOH	0.0036		3

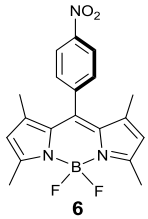 6	CH_3CN	0.0043		3
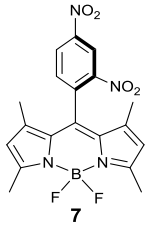 7	hexane	0.021	A = DPIBF; S = MeSBDPI$_2$; λ_{exc} = 509 nm; [O_2] = air	3
	EtOAc	0.026		3
	THF	0.026		3
	pinacolone	0.073		3
	acetone	0.012		3
	MeOH	0.0055		3
	CH_3CN	0.0049		3
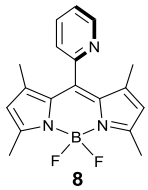 8	hexane	0.0052	A = DPIBF; S = MeSBDPI$_2$; λ_{exc} = 509 nm; [O_2] = air	3
	EtOAc	0.0039		3
	THF	0.012		3
	pinacolone	0.012		3
	acetone	0.012		3
	MeOH	0.013		3
	CH_3CN	0.024		3
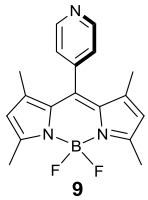 9	hexane	0.0091	A = DPIBF; S = MeSBDPI$_2$; λ_{exc} = 509 nm; [O_2] = air	3
	EtOAc	0.032		3
	THF	0.024		3
	pinacolone	0.020		3
	acetone	0.031		3
	MeOH	0.012		3
	CH_3CN	0.037		3
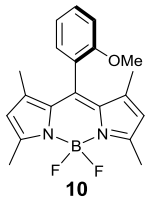 10	hexane	0.029	A = DPIBF; S = MeSBDPI$_2$; λ_{exc} = 509 nm; [O_2] = air	5
	EtOAc	0.057		5
	THF	0.061		5
	pinacolone	0.078		5
	acetone	0.17		5
	MeOH	0.021		5
	CH_3CN	0.18		5
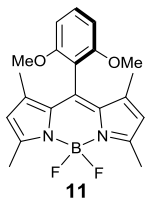 11	hexane	0.040	A[a] = DPIBF; S[b] = MeSBDPI$_2$; λ_{exc} = 509 nm; [O_2][c] = air	5
	EtOAc	0.073		5
	THF	0.051		5
	pinacolone	0.081		5
	acetone	0.082		5
	MeOH	0.036		5
	CH_3CN	0.18		5
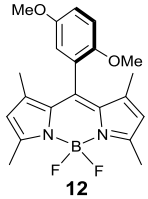 12	hexane	0.026	A = DPIBF; S = MeSBDPI$_2$; λ_{exc} = 509 nm; [O_2] = air	6
	EtOAc	0.178		6
	THF	0.462		6
	pinacolone	0.680		6
	acetone	0.250		6
	MeOH	0.023		6
	CH_3CN	0.125		6
	hexane	0.114	A = DPIBF; S = MeSBDPI$_2$; λ_{exc} = 509 nm; [O_2] = air	6
	EtOAc	0.291		6
	THF	0.357		6

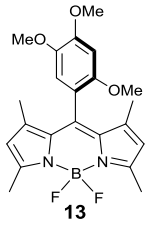 13	pinacolone	0.392		6
	acetone	0.068		6
	MeOH	0.004		6
	CH_3CN	0.033		6
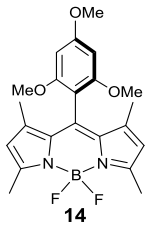 14	hexane	0.024	A = DPIBF; S = MeSBDPI$_2$; λ_{exc} = 509 nm; [O_2] = air	5
	EtOAc	0.063		5
	THF	0.059		5
	pinacolone	0.16		5
	acetone	0.11		5
	MeOH	0.074		5
	CH_3CN	0.31		5
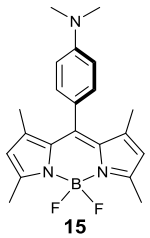 15	hexane	0.102	A = DPIBF; S = MeSBDPI$_2$; λ_{exc} = 509 nm; [O_2] = air	7
	EtOAc	0.412		7
	THF	0.623		7
	pinacolone	0.490		7
	acetone	0.114		7
	MeOH	0.073		7
	CH_3CN	0.062		7
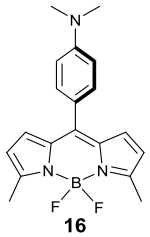 16	hexane	0.23	A = DPIBF; S = MeSBDPI$_2$; λ_{exc} = 509 nm; [O_2] = air	7
	EtOAc	0.171		7
	THF	0.321		7
	pinacolone	0.439		7
	acetone	0.087		7
	MeOH	0.019		7
	CH_3CN	0.052		7
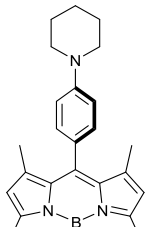 17	hexane	0.058	A = DPIBF; S = MeSBDPI$_2$; λ_{exc} = 509 nm; [O_2] = air	7
	EtOAc	0.511		7
	THF	0.612		7
	pinacolone	0.644		7
	acetone	0.145		7
	MeOH	0.037		7
	CH_3CN	0.083		7
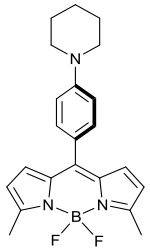 18	hexane	0.258	A = DPIBF; S = MeSBDPI$_2$; λ_{exc} = 509 nm; [O_2] = air	7
	EtOAc	0.220		7
	THF	0.401		7
	pinacolone	0.457		7
	acetone	0.099		7
	MeOH	0.046		7
	CH_3CN	0.057		7
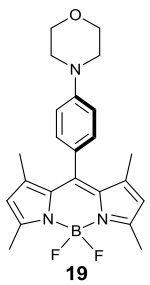 19	hexane	0.120	A = DPIBF; S = MeSBDPI$_2$; λ_{exc} = 509 nm; [O_2] = air	7
	EtOAc	0.676		7
	THF	0.535		7
	pinacolone	0.588		7
	acetone	0.192		7
	MeOH	0.038		7
	CH_3CN	0.083		7
	hexane	0.225		7

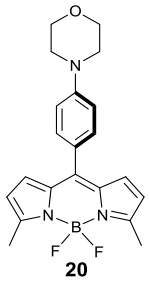 **20**	EtOAc	0.290	A = DPIBF; S = MeSBDPI$_2$; λ_{exc} = 509 nm; [O_2] = air	7
	THF	0.338		7
	pinacolone	0.281		7
	acetone	0.100		7
	MeOH	0.008		7
	CH_3CN	0.033		7
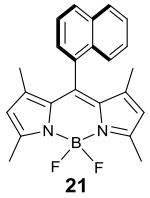 **21**	hexane	0.05	A = DPIBF; S = MeSBDPI$_2$; λ_{exc} = 540 nm; [O_2] = air	4
	toluene	0.043		4
	THF	0.13		4
	EtOH	0.041		4
	CH_3CN	0.057		4
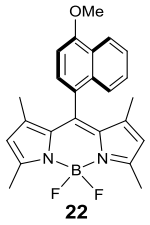 **22**	hexane	0.011	A = DPIBF; S = MeSBDPI$_2$; λ_{exc} = 509 nm; [O_2] = air	6
	EtOAc	0.165		6
	THF	0.232		6
	pinacolone	0.460		6
	acetone	0.471		6
	MeOH	0.274		6
	CH_3CN	0.872		6
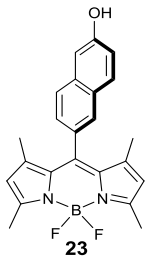 **23**	hexane	0.047	A = DPIBF; S = MeSBDPI$_2$; λ_{exc} = 509 nm; [O_2] = air	6
	EtOAc	0.104		6
	THF	0.442		6
	pinacolone	0.382		6
	acetone	0.111		6
	MeOH	0.131		6
	CH_3CN	0.081		6
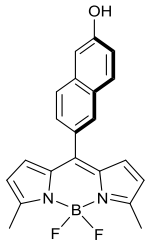 **24**	hexane	0.116	A = DPIBF; S = MeSBDPI$_2$; λ_{exc} = 509 nm; [O_2] = air	6
	EtOAc	0.106		6
	THF	0.19		6
	pinacolone	0.317		6
	acetone	0.070		6
	MeOH	0.046		6
	CH_3CN	0.011		6
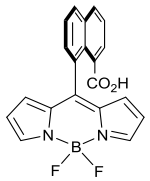 **25**	hexane	n.d.	A = DPIBF; S = MeSBDPI$_2$; λ_{exc} = 540 nm; [O_2] = air	2
	toluene	0.066		2
	CCl_4	0.15		2
	CH_2Cl_2	0.20		2
	THF	0.15		2
	EtOH	0.30		2
	CH_3CN	0.084		2
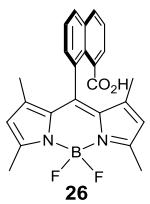 **26**	hexane	0.066	A = DPIBF; S = MeSBDPI$_2$; λ_{exc} = 540 nm; [O_2] = air	2
	toluene	0.038		2
	CCl_4	0.061		2
	CH_2Cl_2	0.068		2
	THF	0.066		2
	EtOH	0.18		2
	CH_3CN	0.092		2
	hexane	0.01	A = DPIBF; S = RB; λ_{exc} = 532 nm; [O_2] = air	8

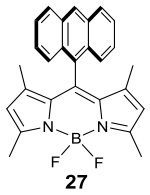 27	toluene	0.045	A = DPIBF; S = MeSBDPI$_2$; λ_{exc} = 540 nm; [O_2] = air	4
	THF	0.21	A = DPIBF; S = MeSBDPI$_2$; λ_{exc} = 540 nm; [O_2] = air	4
	EtOH	0.53	A = DPIBF; S = RB; λ_{exc} = 532 nm; [O_2] = air	8
	CH_3CN	0.22	A = DPIBF; S = MeSBDPI$_2$; λ_{exc} = 540 nm; [O_2] = air	4
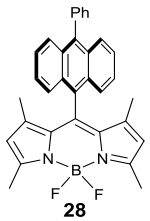 28	hexane	0.04	A = DPIBF; S = RB; λ_{exc} = 532 nm; [O_2] = air	8
	toluene	0.10	A = DPIBF; S = BDPI$_2$; λ_{exc} = n.r.[d]; [O_2] = air[e]	9
	EtOH	0.59	A = DPIBF; S = RB; λ_{exc} = 532 nm; [O_2] = air	8
	CH_3CN	0.84	A = DPIBF; S = BDPI$_2$; λ_{exc} = n.r.[d]; [O_2] = air[e]	9
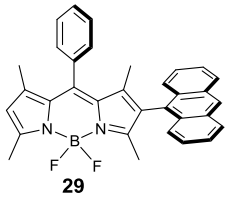 29	toluene	0.20	A = DPIBF; S = BDPI$_2$; λ_{exc} = n.r.[d]; [O_2] = air[e]	9
	CH_2Cl_2	0.24		9
	CH_3CN	0.11		9
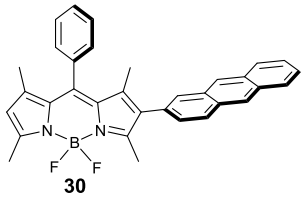 30	toluene	0.11	A = DPIBF; S = BDPI$_2$; λ_{exc} = n.r.[d]; [O_2] = air[e]	9
	CH_2Cl_2	0.13		9
	CH_3CN	0.005		9
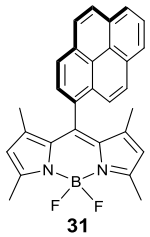 31	hexane	0.01	A = DPIBF; S = RB; λ_{exc} = 532 nm; [O_2] = air	10
	toluene	0.086	A = DPIBF; S = MeSBDPI$_2$; λ_{exc} = 540 nm; [O_2] = air	4
	THF	0.20		4
	EtOH	0.34	A = DPIBF; S = RB; λ_{exc} = 532 nm; [O_2] = air	10
	CH_3CN	0.34	A = DPIBF; S = MeSBDPI$_2$; λ_{exc} = 540 nm; [O_2] = air	4
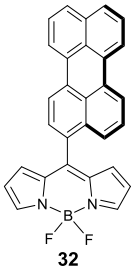 32	hexane	0.1	A = DPIBF; S = BDPI$_2$; λ_{exc} = n.r.[d]; [O_2] = air[e]	11
	toluene	0.31	A = DPIBF; S = BDPI$_2$; λ_{exc} = n.r.[d]; [O_2] = air[e]	12
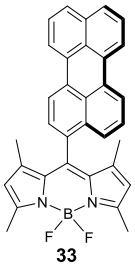 33	toluene	0.18	A = DPIBF; S = BDPI$_2$; λ_{exc} = n.r.[d]; [O_2] = air[e]	11
	THF	0.21		11
	CH_2Cl_2	0.42		11
	CH_3CN	0.11		11
	hexane	0.349		13

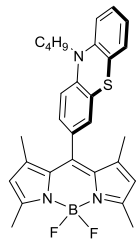 **34**	toluene	0.673	A = DPIBF; S = $BDPI_2$; λ_{exc} = n.r.[d]; $[O_2]$ = air[e]	13
	CH_2Cl_2	0.013		13
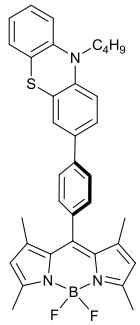 **35**	hexane	0.018	A = DPIBF; S = $BDPI_2$; λ_{exc} = n.r.[d]; $[O_2]$ = air[e]	13
	toluene	0.246		13
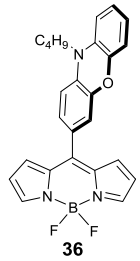 **36**	hexane	0.28	A = DPIBF; S = $BDPI_2$; λ_{exc} = n.r.[d]; $[O_2]$ = air[e]	14
	toluene	0.08		14
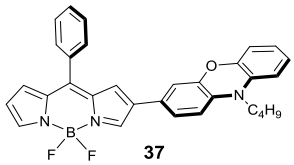 **37**	toluene	0.02	A = DPIBF; S = $BDPI_2$; λ_{exc} = n.r.[d]; $[O_2]$ = air[e]	14
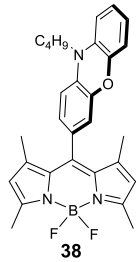 **38**	hexane	0.11	A = DPIBF; S = $BDPI_2$; λ_{exc} = n.r.[d]; $[O_2]$ = air[e]	14
	toluene	0.42		14
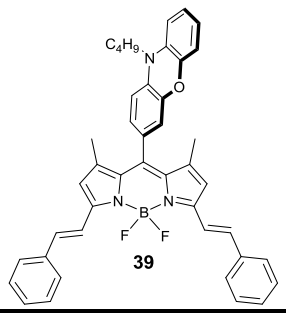 **39**	toluene	0.23	A = DPIBF; S = MB; λ_{exc} = n.r.[d]; $[O_2]$ = air[e]	15
	hexane	0.05		15

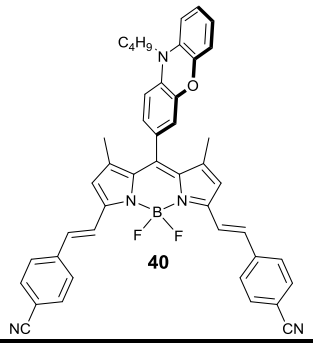 **40**	toluene	0.18	A = DPIBF; S = MB; λ_{exc} = n.r.[d]; $[O_2]$ = air[e]	15
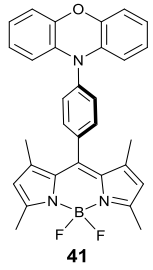 **41**	hexane	0.01	A = DPIBF; S = $BDPI_2$; λ_{exc} = n.r.[d]; $[O_2]$ = air[e]	14
	toluene	0.39		14
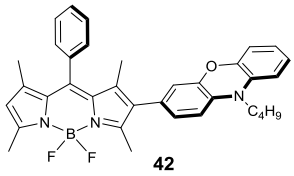 **42**	hexane	0.02	A = DPIBF; S = $BDPI_2$; λ_{exc} = n.r.[d]; $[O_2]$ = air[e]	14
	toluene	0.04		14
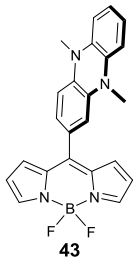 **43**	toluene	0.01	A = DPIBF; S = $BDPI_2$; λ_{exc} = 510 nm; $[O_2]$ = air[e]	16
	THF	0.003		16
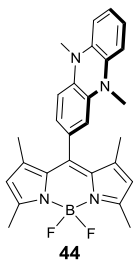 **44**	cyclohexane	0.04	A = DPIBF; S = $BDPI_2$; λ_{exc} = 510 nm; $[O_2]$ = air[e]	16
	toluene	0.014		16
	THF	0.006		16
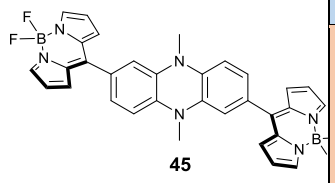 **45**	THF	0.008	A = DPIBF; S = $BDPI_2$; λ_{exc} = 510 nm; $[O_2]$ = air[e]	16
	CH_3CN	0.009		16
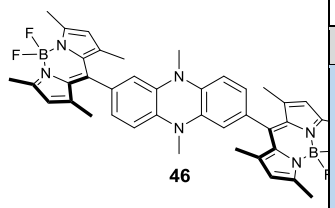 **46**	cyclohexane	0.30	A = DPIBF; S = $BDPI_2$; λ_{exc} = 510 nm; $[O_2]$ = air[e]	16
	toluene	0.05		16
	THF	0.004		16
	toluene	0.033		17
	CH_2Cl_2	0.58		17

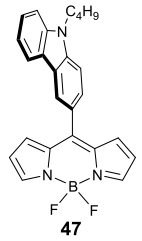 47	CH_3CN	0.024	A = DPIBF; S = $BDPI_2$; λ_{exc} = n.r.; $[O_2]$ = air[e]	17
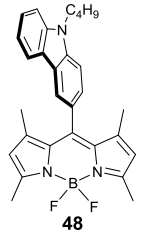 48	toluene	0.023	A = DPIBF; S = $BDPI_2$; λ_{exc} = n.r.; $[O_2]$ = air[e]	17
	CH_2Cl_2	0.082		17
	CH_3CN	0.54		17
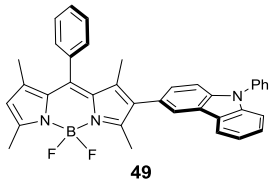 49	toluene	0.083	A = DPIBF; S = $BDPI_2$; λ_{exc} = n.r.; $[O_2]$ = air[e]	17
	CH_2Cl_2	0.026		17
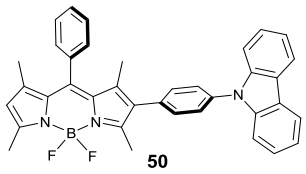 50	toluene	0.09	A = DPIBF; S = $BDPI_2$; λ_{exc} = n.r.; $[O_2]$ = air	18
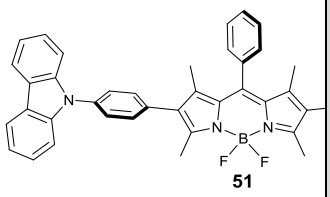 51	toluene	0.11	A = DPIBF; S = $BDPI_2$; λ_{exc} = n.r.; $[O_2]$ = air	18
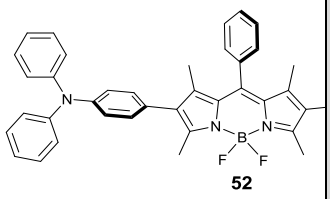 52	toluene	0.19	A = DPIBF; S = $BDPI_2$; λ_{exc} = n.r.; $[O_2]$ = air	18
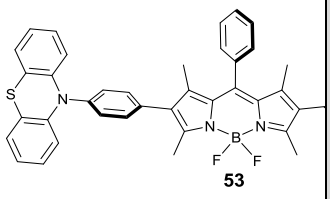 53	toluene	0.32	A = DPIBF; S = $BDPI_2$; λ_{exc} = n.r.; $[O_2]$ = air	18
	CH_2Cl_2	0.022		17

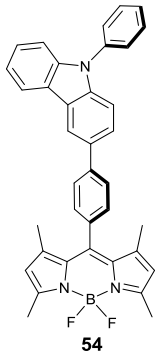 **54**	CH_3CN	0.029	A = DPIBF; S = $BDPI_2$; λ_{exc} = n.r.; $[O_2]$ = air[e]	17
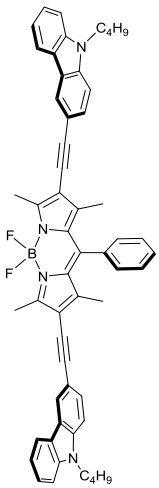 **55**	hexane	0.03	A = DPIBF; S = MB; λ_{exc} = n.r.[d]; $[O_2]$ = air[e]	15
	toluene	0.04		15
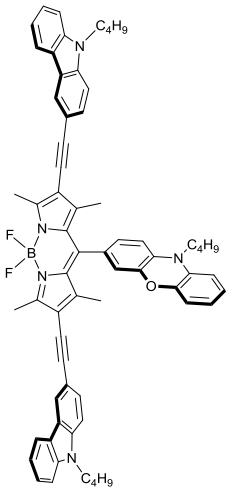 **56**	hexane	0.04	A = DPIBF; S = MB; λ_{exc} = n.r.[d]; $[O_2]$ = air[e]	15
	toluene	0.12		15
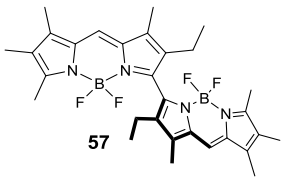 **57**	toluene	0.4	Determined from $^1O_2$ luminescence, using is TPP[f] as a standard; λ_{exc} = 490 nm; $[O_2]$ = air.	19
	CH_2Cl_2	0.5		19
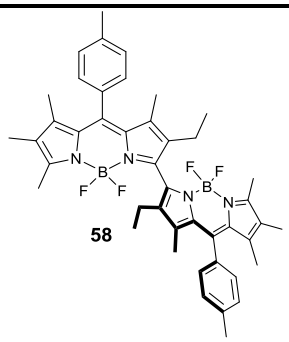 **58**	toluene	0.4	Determined from $^1O_2$ luminescence, using is TPP[f] as a standard; λ_{exc} = 490 nm; $[O_2]$ = air.	19
	CH_2Cl_2	0.5		19

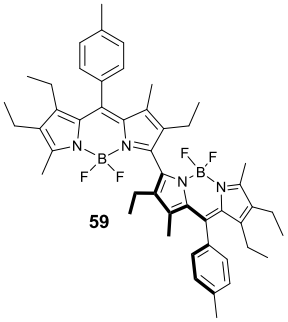 59	toluene	0.3	Determined from $^1O_2$ luminescence, using is TPP[f] as a standard; λ_{exc} = 490 nm; [O_2] = air.	19
	CH_2Cl_2	0.5		19
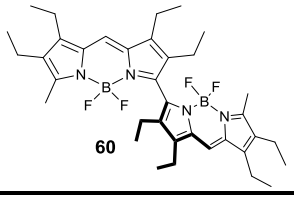 60	toluene	0.3	Determined from $^1O_2$ luminescence, using is TPP[f] as a standard; λ_{exc} = 490 nm; [O_2] = air.	19
	CH_2Cl_2	0.5		19
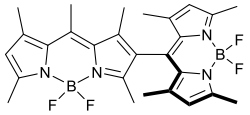 61	toluene	0.24	A = DPIBF; S = MB; λ_{exc} = n.r.[d]; [O_2] = air[e]	20
	$CHCl_3$	0.75	Determined from $^1O_2$ luminescence, using is $MeSBDPI_2$ as a standard; λ_{exc} = 490 nm; [O_2] = air.	21
	THF	0.86		21
	CH_2Cl_2	0.64	A = DPIBF; S = MB; λ_{exc} = n.r.[d]; [O_2] = air[e]	20
	acetone	0.5	Determined from $^1O_2$ luminescence, using is $MeSBDPI_2$ as a standard; λ_{exc} = 490 nm; [O_2] = air.	21
	CH_3CN	0.25		21
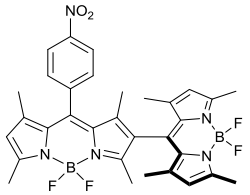 62	toluene	0.44	A = DPIBF; S = MB; λ_{exc} = n.r.[d]; [O_2] = air[e]	20
	CH_2Cl_2	0.20		20
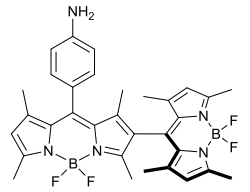 63	toluene	0.144	A = DPIBF; S = MB; λ_{exc} = n.r.[d]; [O_2] = air[e]	20
	CH_2Cl_2	0.68		20
	CH_3CN	0.112		20
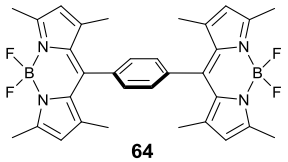 64	toluene	0.01	A = DPIBF; S = MB; λ_{exc} = n.r.[d]; [O_2] = air[e]	20
	CH_2Cl_2	0.09		20
	CH_3CN	0.03		20

[a] Singlet oxygen trapping reagents: DPIBF - 1,3-diphenylisobenzofuran. [b] Reference photosensitizer: MeSBDPI2 - 8-methylthio-2,6-diiodoBODIPY; RB – Rose Bengal; $BPDI_2$ - 2,6-diiodo-1,3,5,7-tetramethyl-8-phenylBODIPY; MB – Methylene Blue. [c] Oxygen concentration. [d] Not reported. [e] Oxygen concentration not given; assumed to be air saturated.

2. Synthetic Procedures and Characterization

2.1 Materials and Instruments

General Information: All reactions were performed in standard round-bottomed flasks under an argon atmosphere. All commercial reagents and solvents were used as received without further purification. Syringes were used for the addition of all liquid reagents. Yields refer to chromatographically and spectroscopically (^{1}H NMR) homogeneous material, unless otherwise noted. Reactions were monitored by thin layer chromatography (Merck, TLC Silica gel 60 F_{254}) and visualized by UV irradiation (λ = 254 nm). Flash column chromatography was carried out on silica gel 60 *Merck, 230–400 mesh (mobile phases are given as (*v/v*)). Room temperature refers to 20–25 °C.

Instrumentation: Melting points are uncorrected and were measured on a Reichert Thermovar Apparatus. NMR spectra were recorded on a Bruker Advance III 400 MHz spectrometer for ^{1}H (400 MHz), ^{13}C (101 MHz), ^{19}F (377 MHz) and ^{11}B (128 MHz) NMR spectra. All NMR spectra were recorded at 25 ºC. Resonances δ are given in ppm units and referenced to the deuterium peak in the NMR solvent: $CDCl_3$ (δ_H = 7.26 ppm, δ_C = 77.2 ppm). Signal multiplicities are abbreviated as follows: singlet = s, doublet = d, triplet = t, doublet of doublets = dd, multiplet = m. HRMS analyses were acquired in positive modes as required, using a Micromass time-of-flight mass spectrometer (TOF) interfaced to a Waters 2960 HPLC or a Bruker microTOF-Q III spectrometer interfaced to a Dionex UltiMate 3000 LC.

UV-Vis spectra were recorded in solutions using a PerkinElmer Lambda 900 UV/VIS/NIR Spectrometer (1 cm path length quartz cell). Emission spectra were measured using a PerkinElmer LS 55 Luminescence Spectrometer. Emission quantum yields of the compounds were measured relative to the fluorescence of rhodamine 6G in EtOH (Φ_F = 0.95).[22]

Photo-irradiations were performed in quartz cuvettes (1 cm) using a Melles Griot 43 series ion laser (543R-AP-AO1, average intensity of 12 mW cm^{-2}).

2.2 Chemical Synthesis of BDP 1-7

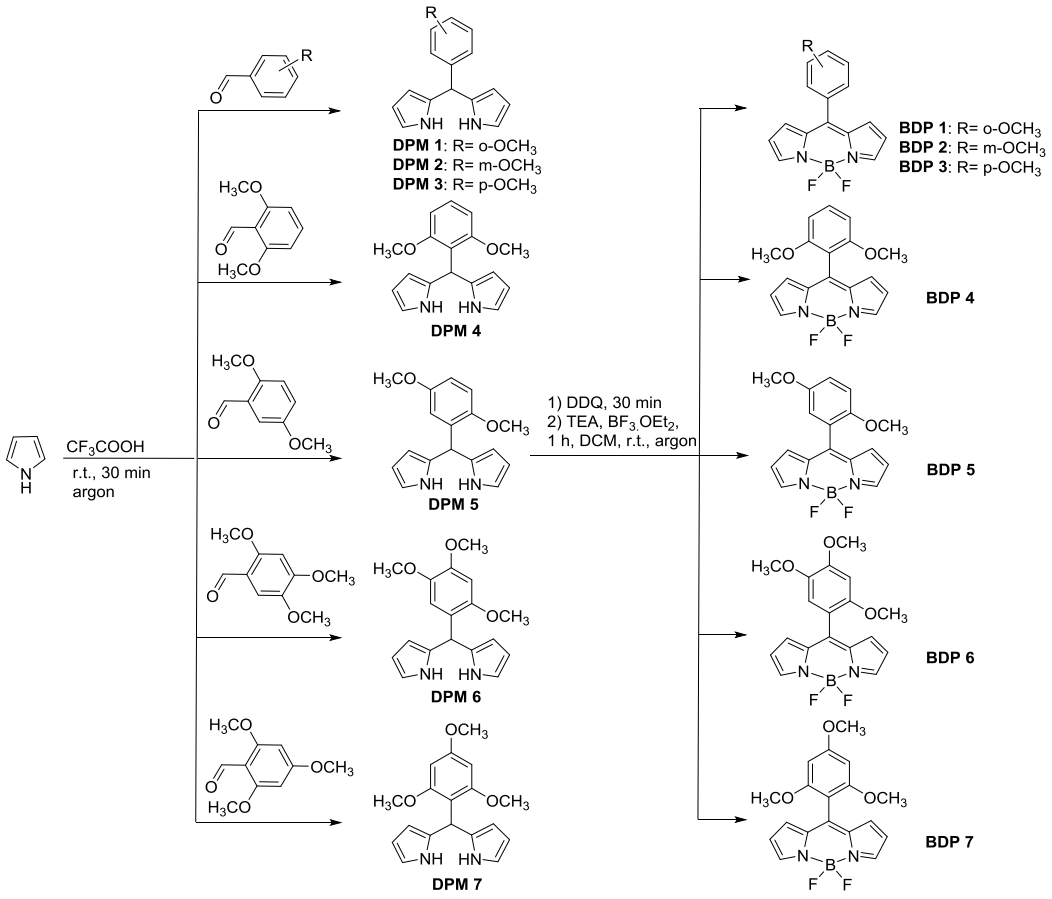

Scheme S1. Synthesis of BODIPY compounds.

General Procedure 1: Dipyrromethane (**DPM 4-7**) (1 equiv) was dissolved in CH_2Cl_2, degassed with an Ar stream for 5 min and oxidized with DDQ (1.2 equiv) for half an hour. To this mixture TEA (40 equiv) and $BF_3{\cdot}OEt_2$ (50 equiv) were added without any time delay under Ar atm. and allowed to stir at room temperature for 1 h. After 1 h, extractions were carried out with water and the organic extract was collected, dried with anhydrous Na_2SO_4 and the solvents were removed under reduced pressure. The crude products were subjected to silica gel column chromatography in order to obtain the desired pure compounds.

BDP 4. Synthesized via General Procedure 1 from dipyrromethane (**DPM 4**) (200 mg, 0.71 mmol), DDQ (193 mg, 0.85 mmol), TEA (3.9 mL, 28.32 mmol) and TFA (4.4 mL, 35.4 mmol) in 90 mL CH_2Cl_2. The crude material was purified by silica gel column chromatography. Desired product was eluted with (70/30) CH_2Cl_2/hexane mixture. Final purification was performed through recrystallization in a MeOH/H_2O mixture giving **BDP 4** as a green solid. Yield= 160 mg of **BDP 4** (0.49 mmol, 69%). m.p. = 131-140 °C; R_f = 0.50 (SiO_2, CH_2Cl_2/hexane, 7:3, v/v); ^{1}H NMR (400 MHz, $CDCl_3$): δ = 7.86 (s, 2H), 7.41 (t, J = 8.4 Hz, 1H), 6.74 (d, J = 4.1 Hz, 2H), 6.66 (d, J = 8.4 Hz, 2H), 6.43 (d, J = 3.0 Hz, 2H), 3.69 ppm (s, 6H); ^{13}C NMR (101 MHz, $CDCl_3$): δ = 158.59, 143.60, 136.37, 131.45, 130.37, 117.98, 111.03, 104.00, 56.09 ppm; ^{19}F NMR (377 MHz, $CDCl_3$) : δ = δ -145.33 ppm (dd, J = 58.4, 29.1 Hz, 2 F); ^{11}B NMR (128 MHz, $CDCl_3$): δ = 0.34 ppm (t, J = 28.8 Hz); UV-Vis (CH_2Cl_2): λ_{max} {log (ε [L mol^{-1} cm^{-1}])} = 507 nm (4.75); HRMS (ESI-QTOF): *m/z* calcd for $C_{17}H_{15}BF_2N_2NaO_2$ $[M+Na]^+$ 351.108996; found 351.108910.

BDP 5. Synthesized via General Procedure 1 from **DPM 5** (200 mg, 0.71 mmol), DDQ (193 mg, 0.85 mmol), TEA (3.9 mL, 28.32 mmol) and TFA (4.4 mL, 35.4 mmol) in 90 mL CH_2Cl_2. The crude material was purified by silica gel column chromatography. Desired product was eluted with (60/40) CH_2Cl_2/hexane mixture. Final purification was performed through recrystallization in a MeOH/H_2O mixture giving **BDP 5** as an orange powder. Yield= 152 mg of **BDP 5** (0.46 mmol, 65%). m.p. = 108-110 °C; R_f = 0.55 (SiO_2, CH_2Cl_2/hexane, 3:2, v/v); ^{1}H NMR (400 MHz, $CDCl_3$): δ = 7.89 (s, 2H), 7.03 (dd, J = 9.0, 3.0 Hz, 1H), 6.97 (d, J = 9.0 Hz, 1H), 6.88 (d, J = 3.0 Hz, 1H), 6.83 (d, J = 4.0 Hz, 2H), 6.48 (d, J = 3.3 Hz, 2H), 3.79 (s, 3H), 3.69 (s, 3H) ppm; ^{13}C NMR (101 MHz, $CDCl_3$): δ = 153.16, 151.40, 144.11, 135.75, 131.30, 123.26, 118.38, 117.40, 116.58, 112.87, 56.45, 56.00 ppm; ^{19}F NMR (377 MHz, $CDCl_3$): δ = -144.37 (m, 1 F), -146.09 (m, 1 F) ppm; ^{11}B NMR (128 MHz, $CDCl_3$): δ = 0.29 (t, J = 28.7 Hz) ppm; UV-Vis (CH_2Cl_2): λ_{max} {log (ε [L mol^{-1} cm^{-1}])} = 506 nm (4.85); HRMS (ESI-QTOF): *m/z* calcd for $C_{17}H_{15}BF_2N_2NaO_2$ $[M+Na]^+$ 351.108996; found 351.108698.

BDP 6. Synthesized via General Procedure 1 from dipyrromethane (**DPM 6**) (200 mg, 0.64 mmol), DDQ (175 mg, 0.77 mmol), TEA (3.6 mL, 25.61 mmol) and TFA (3.9 mL, 32.01 mmol) in 80 mL CH_2Cl_2. The crude material was purified by silica gel column chromatography. Desired product was eluted with (90/10) CH_2Cl_2/hexane mixture. Final purification was performed through recrystallization in a MeOH/H_2O mixture giving the final BODIPY compound as a green solid. Yield= 200 mg of **BDP 6** (0.56 mmol, 87%). m.p. = 115-124 °C; R_f = 0.46 (SiO_2, CH_2Cl_2/hexane, 9:1, v/v); ^{1}H NMR (400 MHz, $CDCl_3$): δ = 7.88 (s, 2H), 6.91 – 6.81 (m, 3H), 6.64 (s, 1H), 6.49 (dd, J = 4.1, 1.5 Hz, 2H), 3.99 (s, 3H), 3.83 (s, 3H), 3.72 (s, 3H) ppm; ^{13}C NMR (101 MHz, $CDCl_3$): δ = 152.11, 151.70, 143.62, 142.87, 135.92, 131.21, 118.20, 115.45, 113.88, 97.84, 56.78, 56.75, 56.33 ppm; ^{19}F NMR (377 MHz, $CDCl_3$): δ = -144.31 (m, 1 F), -146.25 (m, 1 F) ppm; ^{11}B NMR (128 MHz, $CDCl_3$): δ = 0.29 (t, J = 28.8 Hz) ppm; UV-Vis (CH_2Cl_2): λ_{max} {log (ε [L mol^{-1} cm^{-1}])} = 506 nm (4.68); HRMS (ESI-QTOF): *m/z* calcd for $C_{17}H_{15}BF_2N_2NaO_2$ $[M+Na]^+$ 381.119579; found 381.119879.

BDP 7. Synthesized via General Procedure 1 from **DPM 7** (200 mg, 0.64 mmol), DDQ (175 mg, 0.77 mmol), TEA (3.6 mL, 25.61 mmol) and TFA (3.9 mL, 32.01 mmol) in 80 mL CH_2Cl_2. The crude material was purified by silica gel column chromatography. Desired product was eluted with CH_2Cl_2/EtOH (1%) mixture. Final purification was performed through recrystallization in a MeOH/H_2O mixture giving **BDP 7** as an orange solid. Yield= 125 mg of **BDP 7** (0.35 mmol, 55%. m.p. = 114-126 °C; R_f = 0.60 (SiO_2, CH_2Cl_2/EtOH, 9.9:0.1, v/v); ^{1}H NMR (400 MHz, $CDCl_3$): δ = 7.84 (s, 2H), 6.76 (d, J = 4.2 Hz, 2H), 6.46 – 6.38 (m, 2H), 6.21 (s, 2H), 3.89 (s, 3H), 3.67 (s, 6H) ppm; ^{13}C NMR (101 MHz, $CDCl_3$): δ = 162.89, 159.43, 143.30, 136.79, 130.42, 117.86, 103.92, 90.77, 56.01, 55.62 ppm; ^{19}F NMR (377 MHz, $CDCl_3$): δ = -145.36 (dd, J = 58.5, 29.0 Hz, 2 F) ppm; ^{11}B NMR (128 MHz, $CDCl_3$): δ = 0.33 (t, J = 28.9 Hz) ppm; UV-Vis (CH_2Cl_2):

λ_{max} {log (ε [L mol^{-1} cm^{-1}])} = 507 nm (4.81); HRMS (ESI-QTOF): *m/z* calcd for $C_{17}H_{15}BF_2N_2NaO_2$ $[M+Na]^+$ 381.119579; found 381.119449.

2.3 NMR and HRMS Data

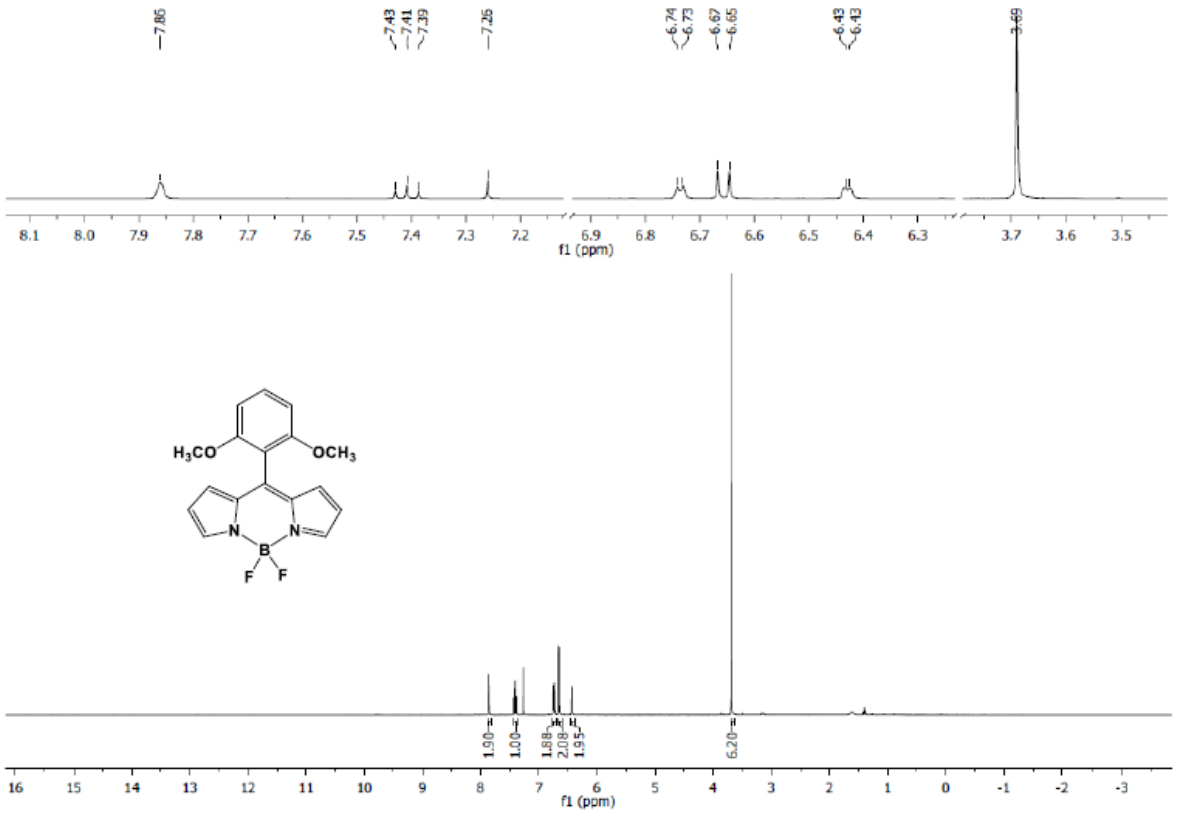

Figure S1. ^{1}H NMR spectrum of **BDP-4** (400 MHz, *CDCl$_3$*, 25 °C).

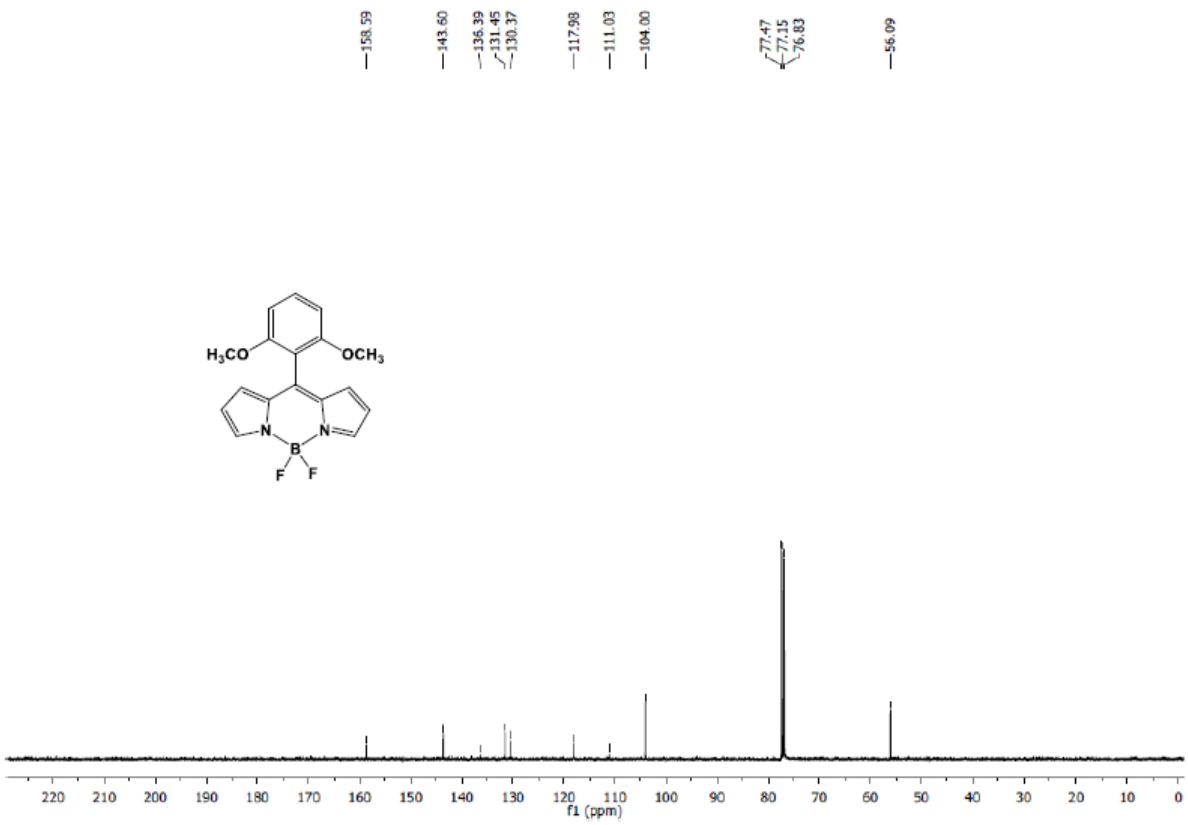

Figure S2. ^{13}C NMR spectrum of **BDP-4** (101 MHz, *CDCl$_3$*, 25 °C).

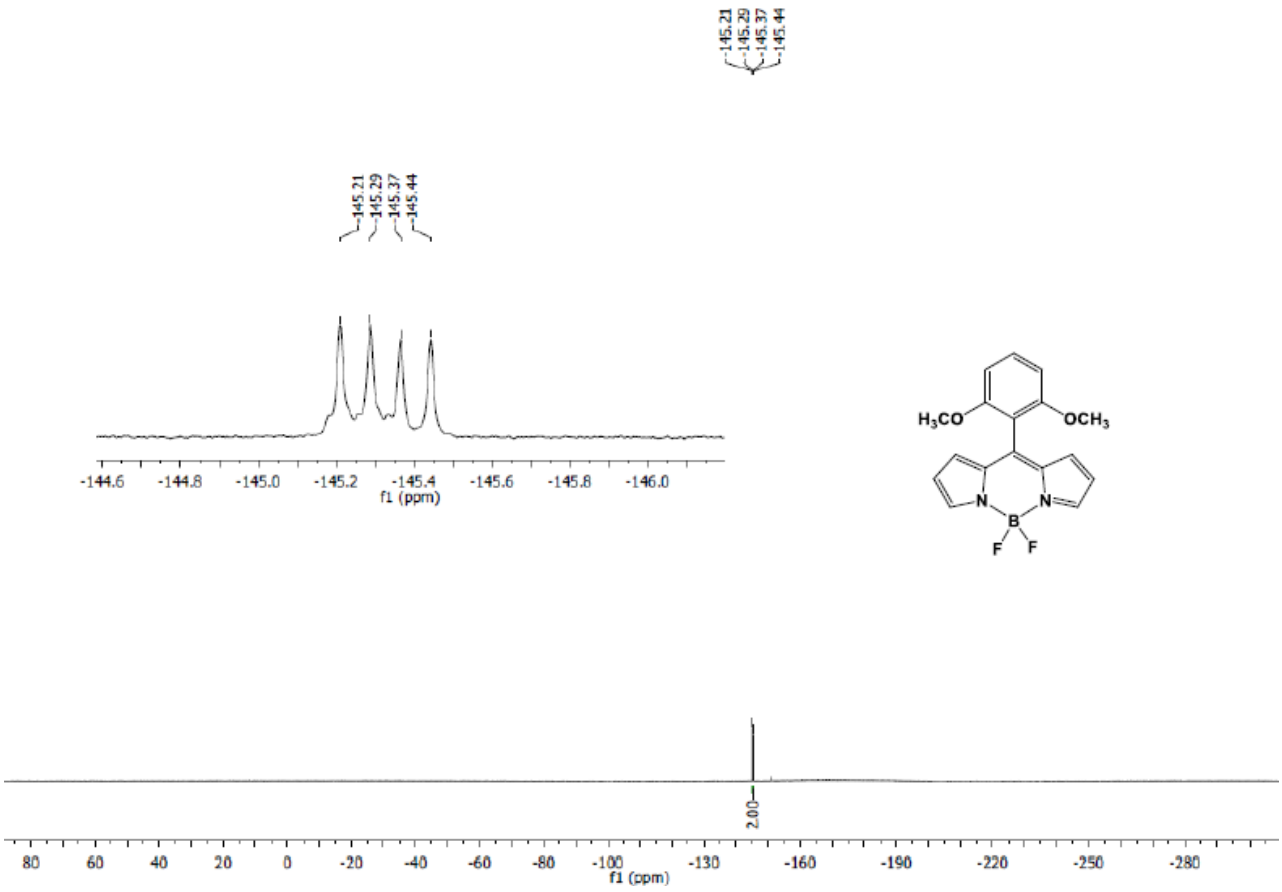

Figure S3. ^{19}F NMR spectrum of **BDP-4** (377 MHz, *$CDCl_3$*, 25 °C).

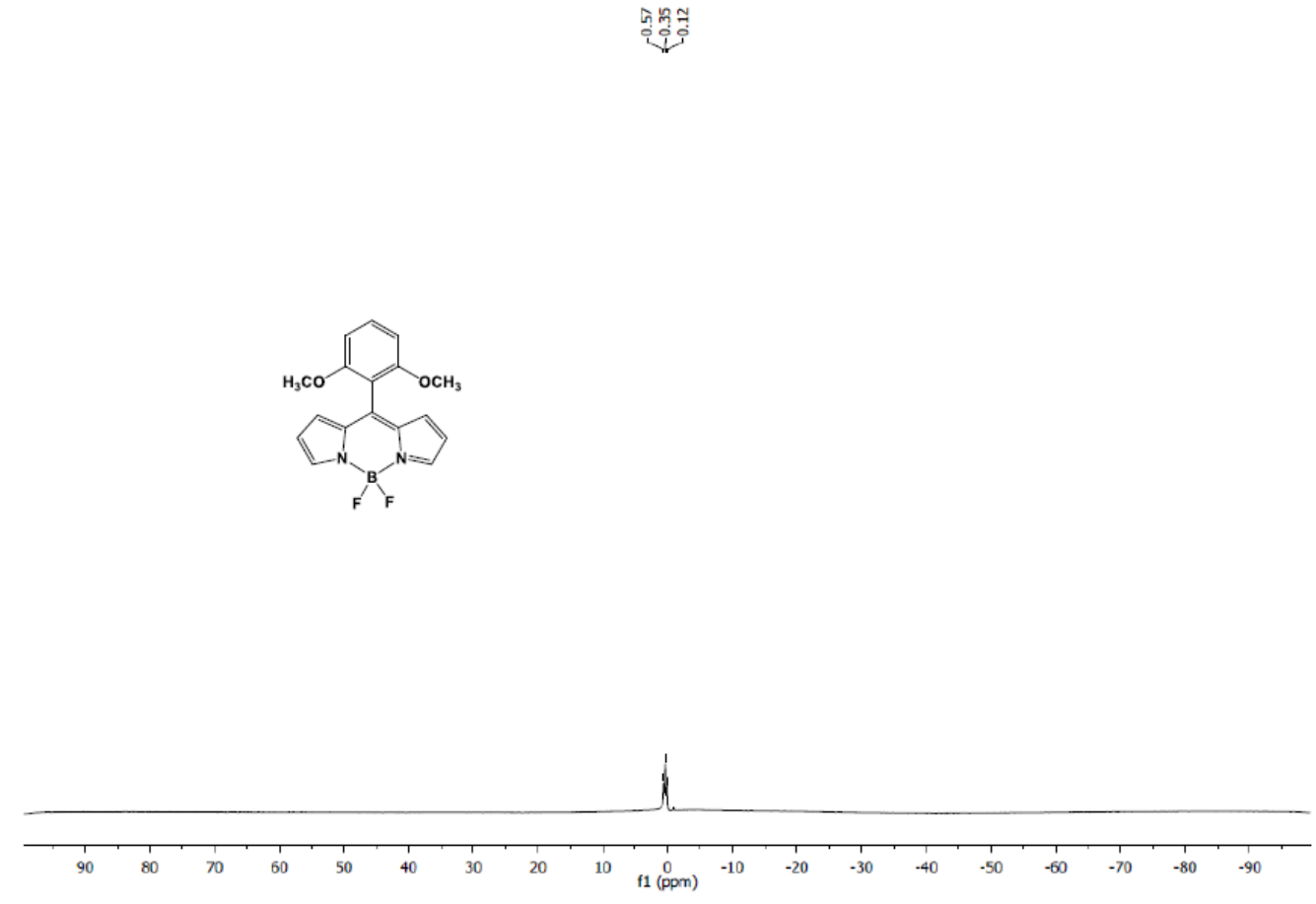

Figure S4. ^{11}B NMR spectrum of **BDP-4** (128 MHz, *$CDCl_3$*, 25 °C).

Sample-ID		Station	
Submitter		Supervisor	
Analysis Name	AST-2020-11_RA6_01_23760.d	Acquisition Date	30/09/2020 11:59:26
Sample Description			

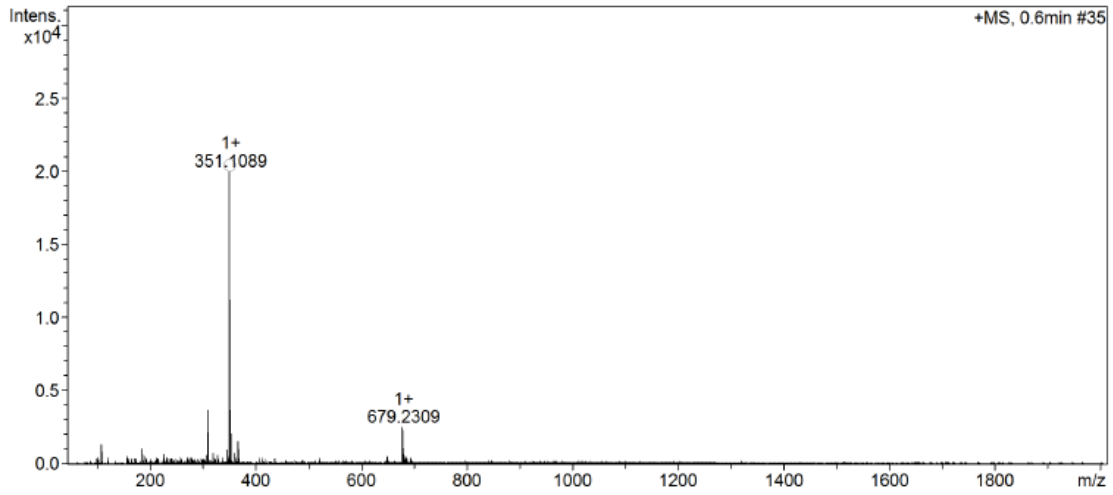

Meas. m/z	#	Ion Formula	m/z	err [mDa]	err [ppm]	rdb	N-Rule	e⁻ Conf	mSigma
351.108910	1	C17H15BF2N2NaO2	351.108996	-0.1	-0.2	10.5	ok	even	5.6

Figure S5. ESI-MS of **BDP-4**.

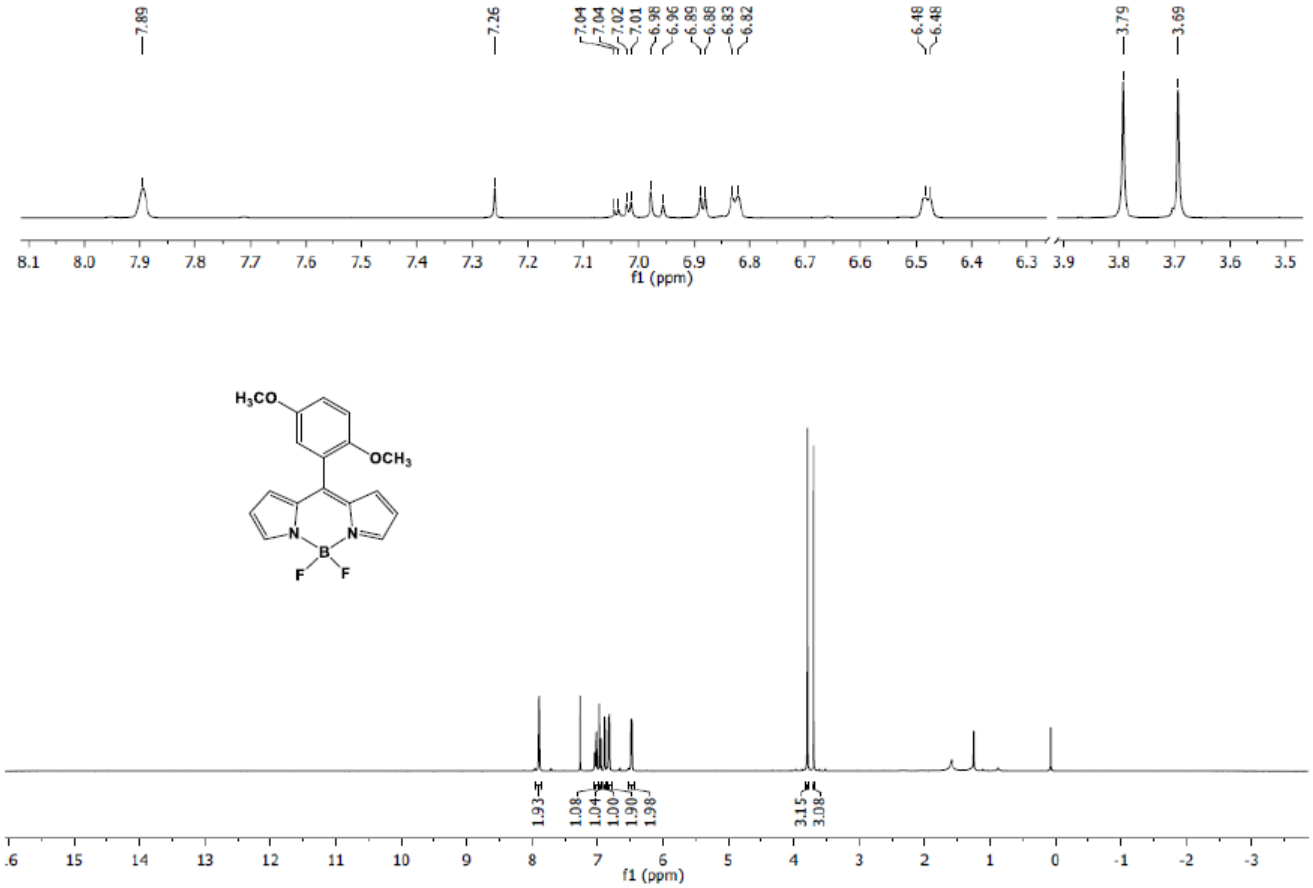

Figure 6. ^{1}H NMR spectrum of **BDP-5** (400 MHz, $CDCl_3$, 25 °C).

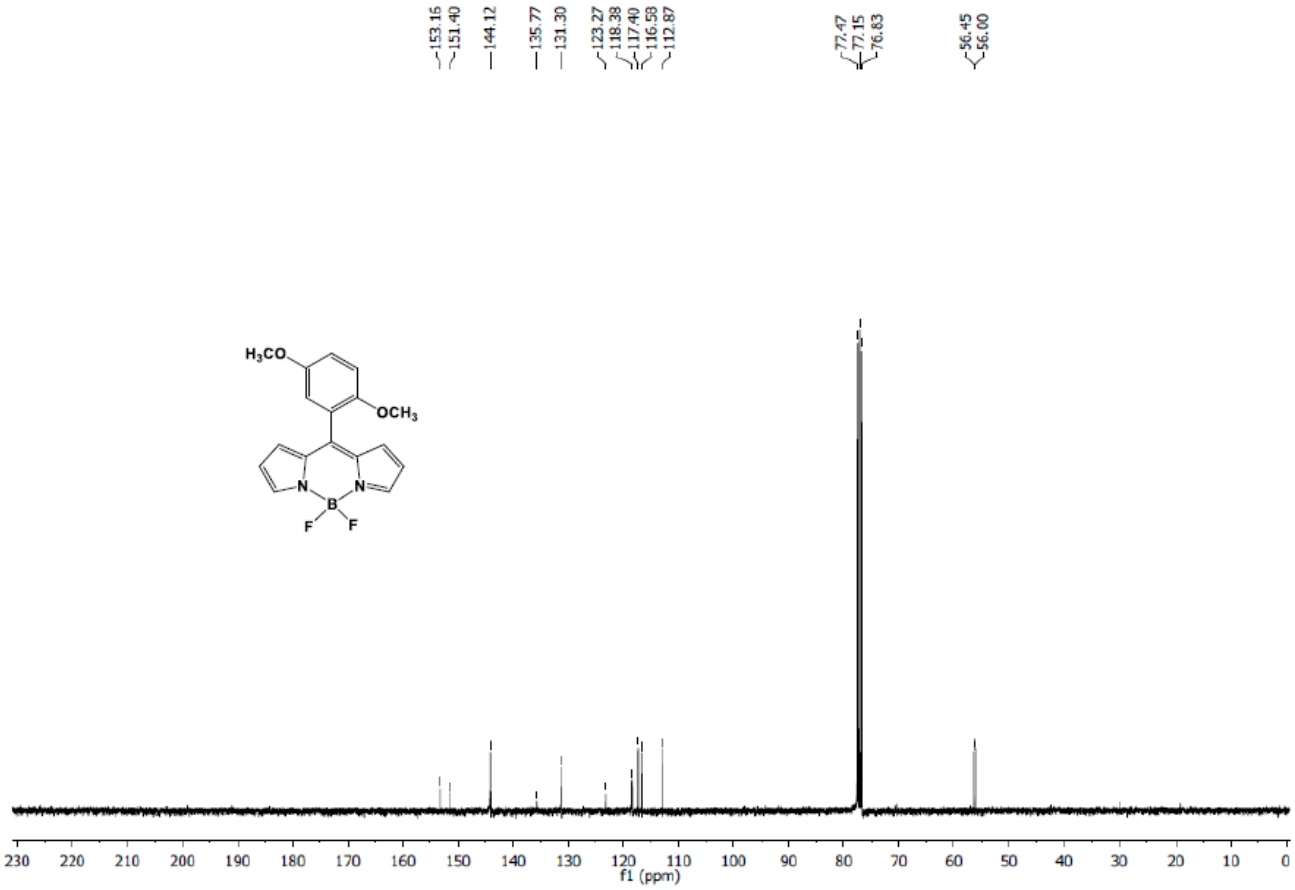

Figure S7. ^{13}C NMR spectrum of **BDP-5** (101 MHz, *$CDCl_3$*, 25 °C).

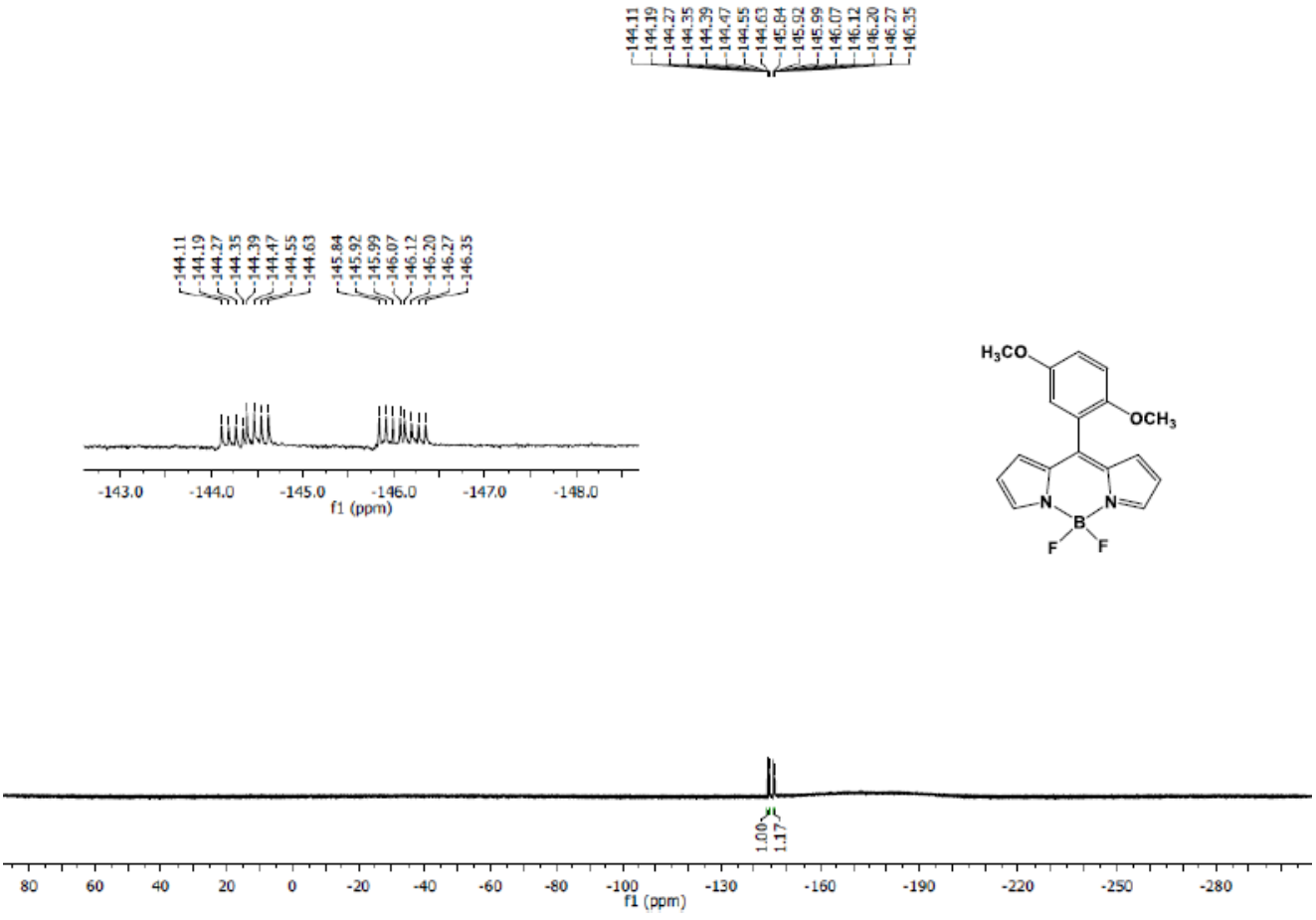

Figure S8. ^{19}F NMR spectrum of **BDP-5** (377 MHz, *$CDCl_3$*, 25 °C).

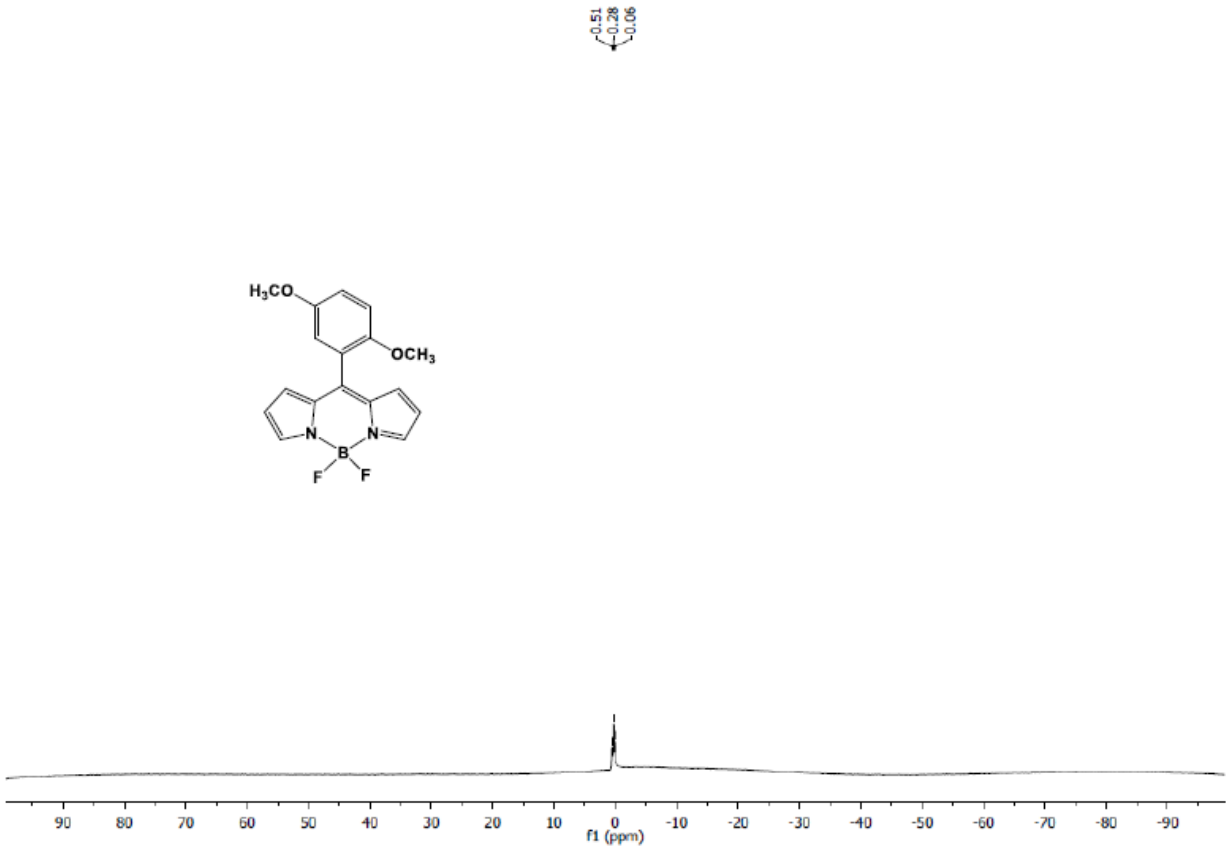

Figure S9. ^{11}B NMR spectrum of **BDP-5** (128 MHz, $CDCl_3$, 25 °C).

Sample-ID		Station	
Submitter		Supervisor	
Analysis Name	AST-2020-12_RA7_01_23761.d	Acquisition Date	30/09/2020 12:02:46
Sample Description			

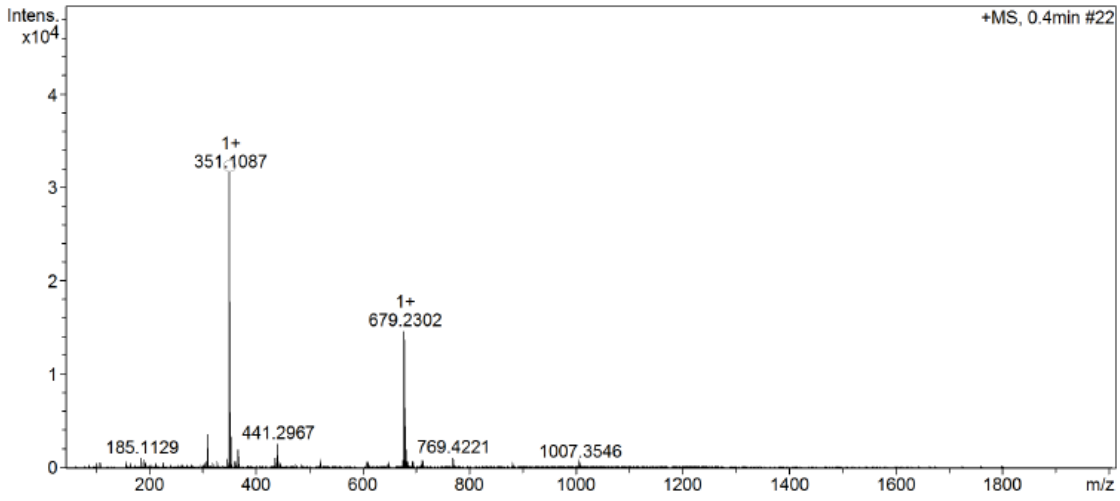

Meas. m/z	#	Ion Formula	m/z	err [mDa]	err [ppm]	rdb	N-Rule	e⁻ Conf	mSigma
351.108698	1	C17H15BF2N2NaO2	351.108996	0.3	0.9	10.5	ok	even	7.9

Figure S10. ESI-MS of **BDP-5**.

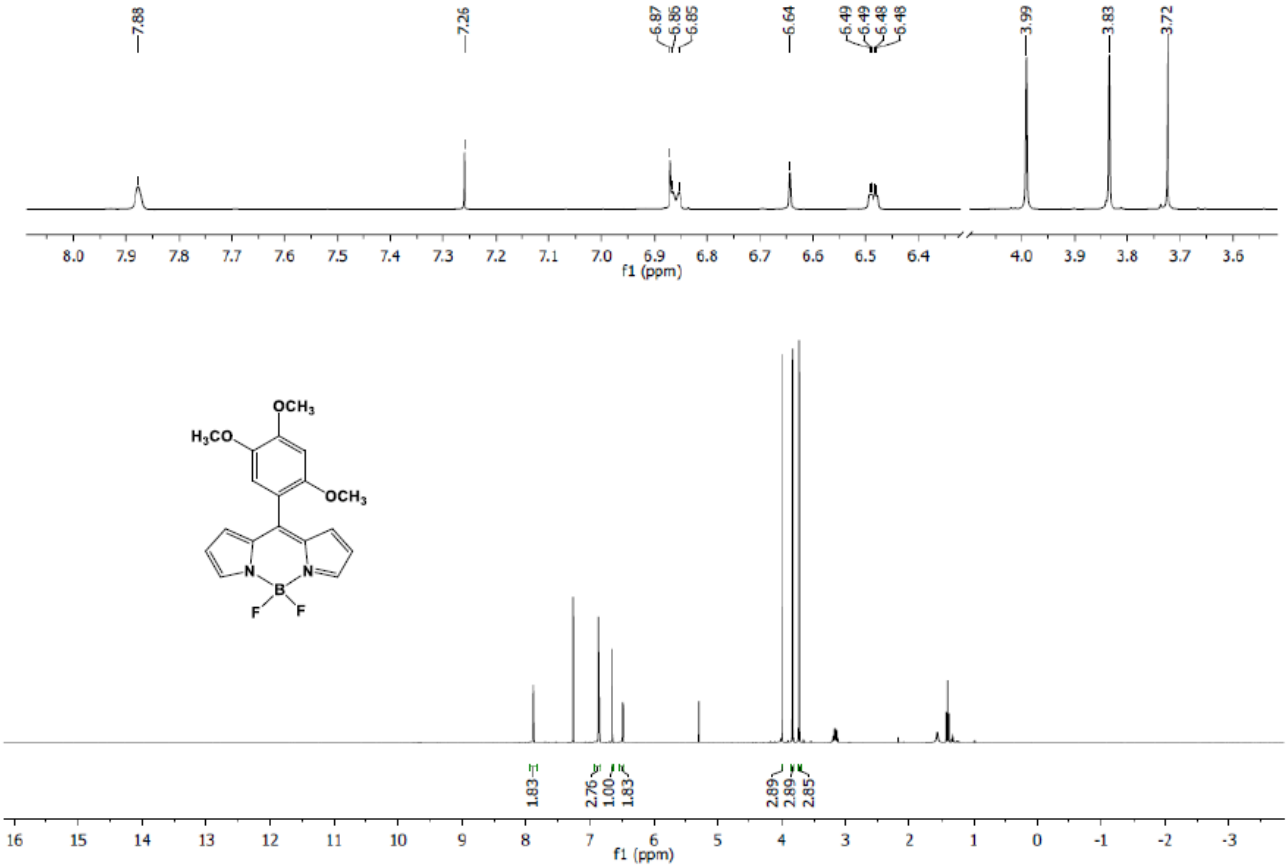

Figure S11. [1]H NMR spectrum of **BDP-6** (400 MHz, *CDCl₃*, 25 °C).

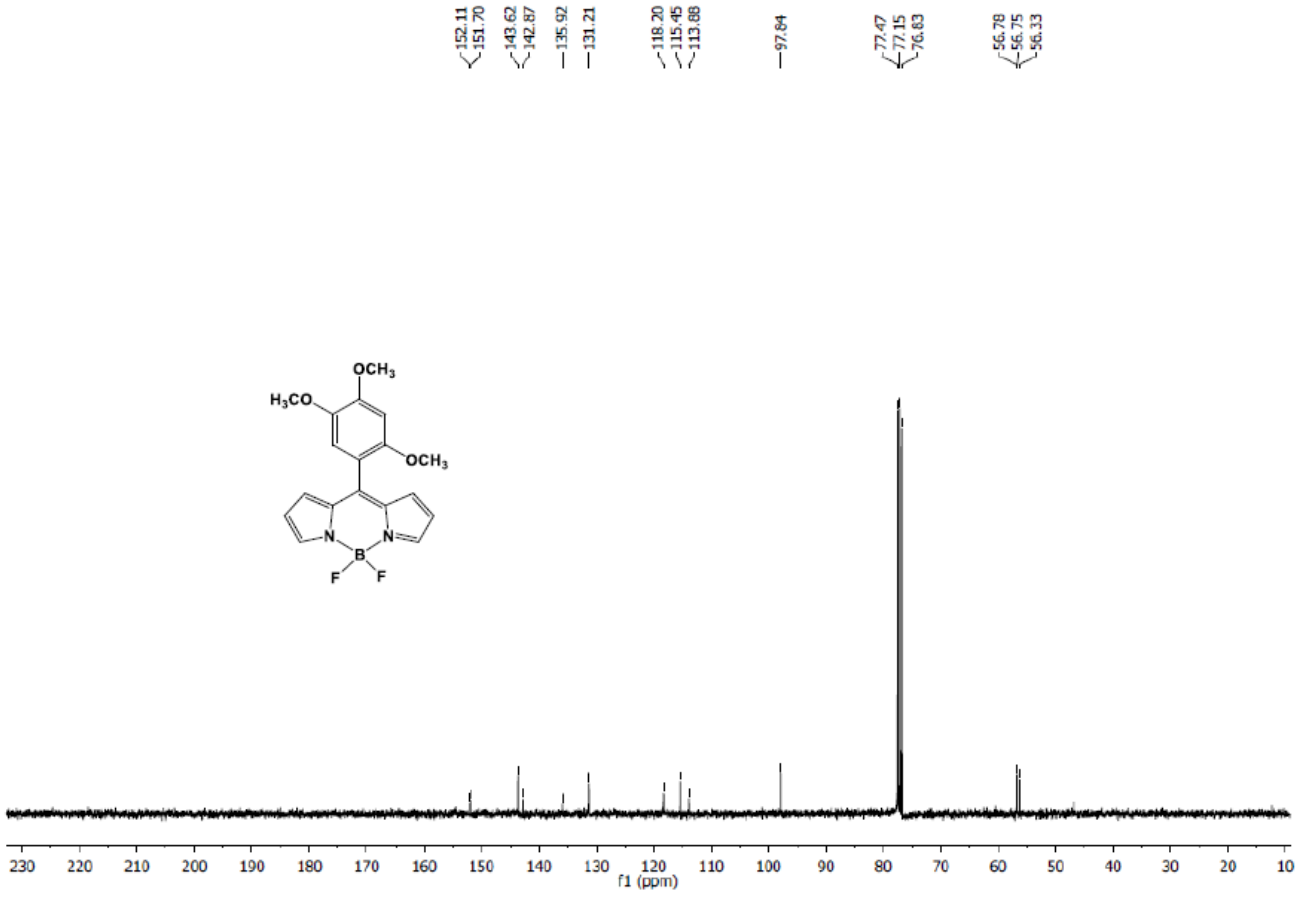

Figure S12. [13]C NMR spectrum of **BDP-6** (101 MHz, *CDCl₃*, 25 °C).

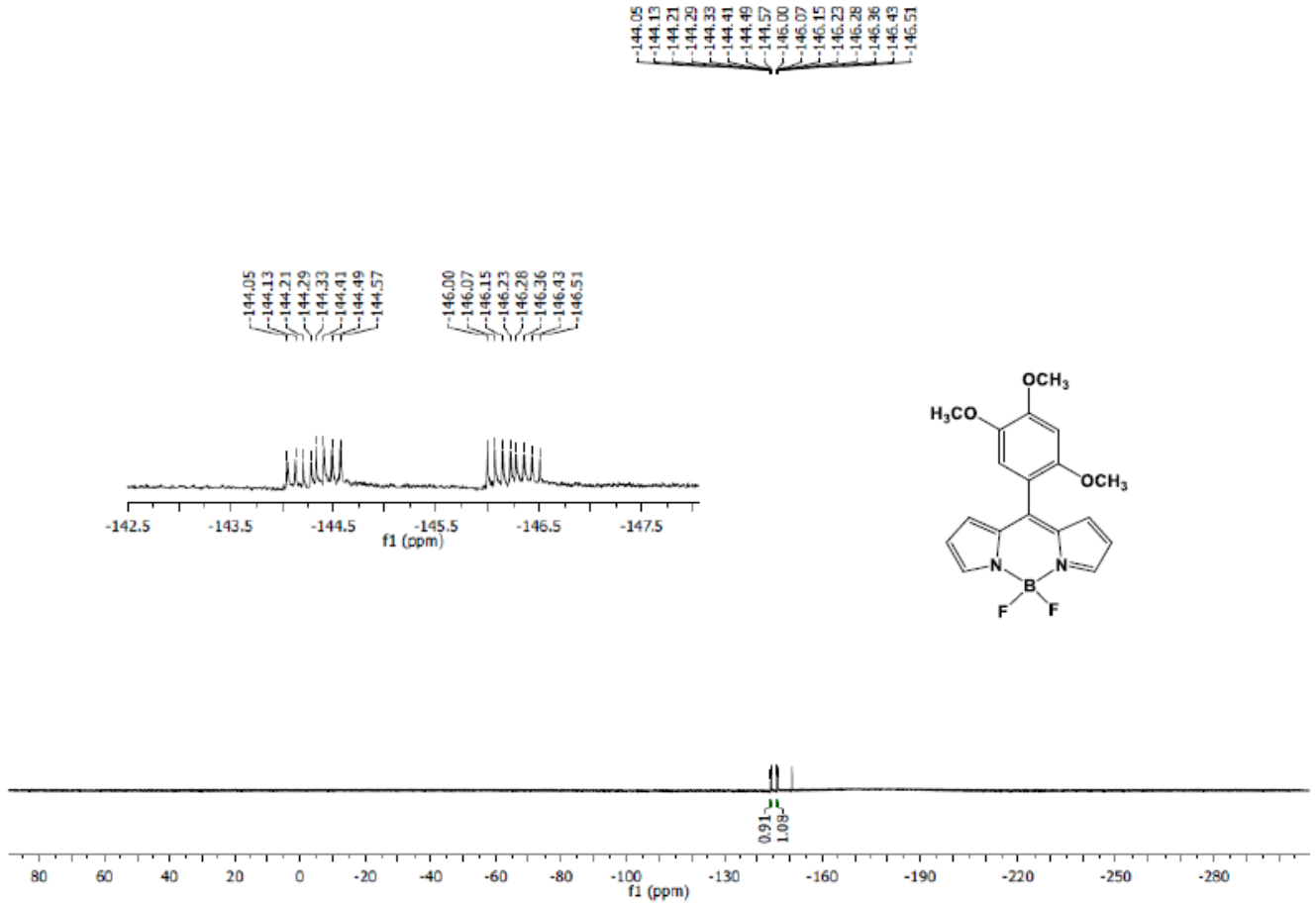

Figure S13. ^{19}F NMR spectrum of **BDP-6** (377 MHz, *$CDCl_3$*, 25 °C).

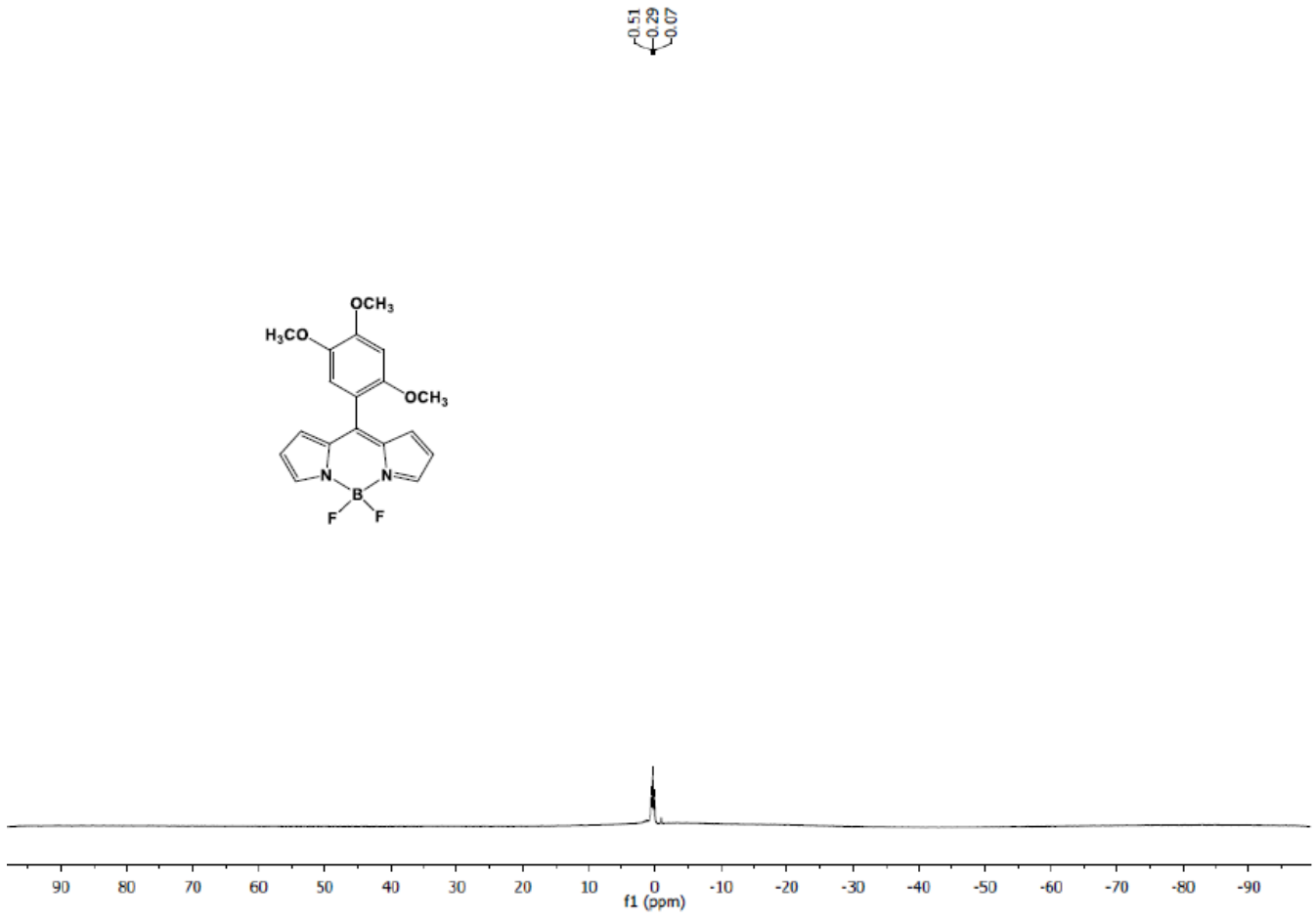

Figure S14. ^{11}B NMR spectrum of **BDP-6** (128 MHz, $CDCl_3$, 25 °C).

Sample-ID		Station	
Submitter		Supervisor	
Analysis Name	AST-2020-13_RA8_01_23762.d	Acquisition Date	30/09/2020 12:06:05
Sample Description			

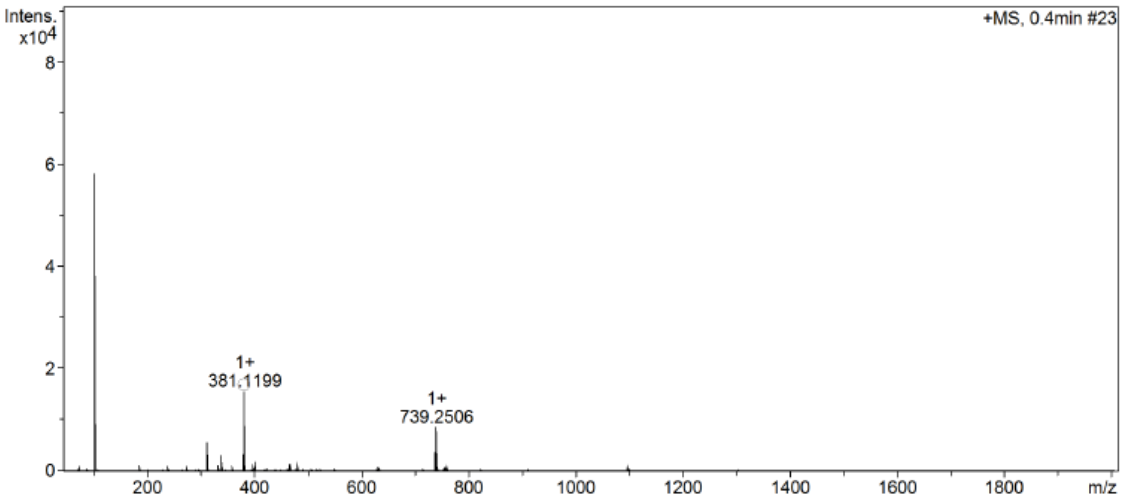

Meas. m/z	#	Ion Formula	m/z	err [mDa]	err [ppm]	rdb	N-Rule	e⁻ Conf	mSigma
381.119879	1	C18H17BF2N2NaO3	381.119579	0.3	0.8	10.5	ok	even	19.3

Figure S15. ESI-MS of **BDP-6**.

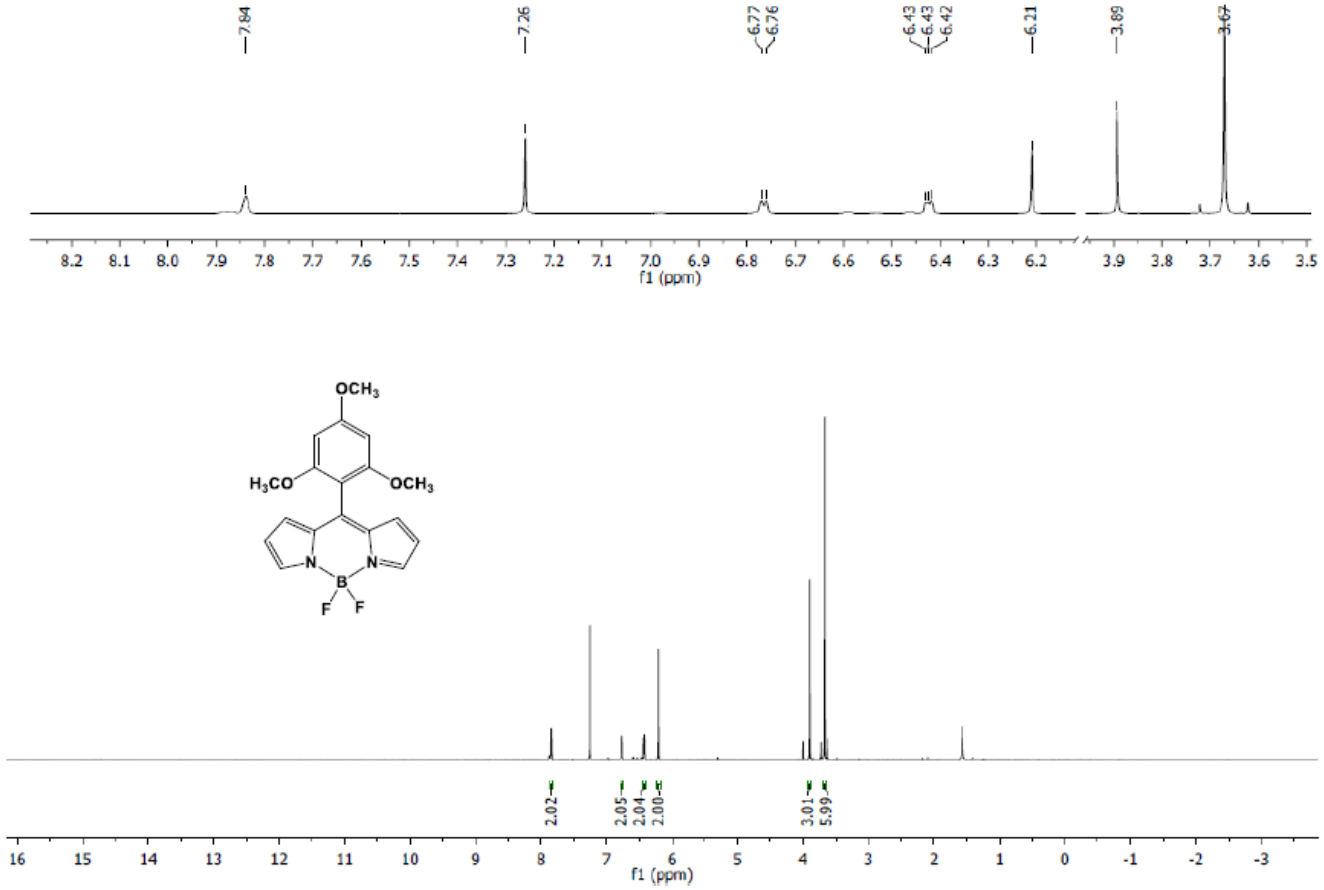

Figure S16. ^{1}H NMR spectrum of **BDP-7** (400 MHz, $CDCl_3$, 25 °C).

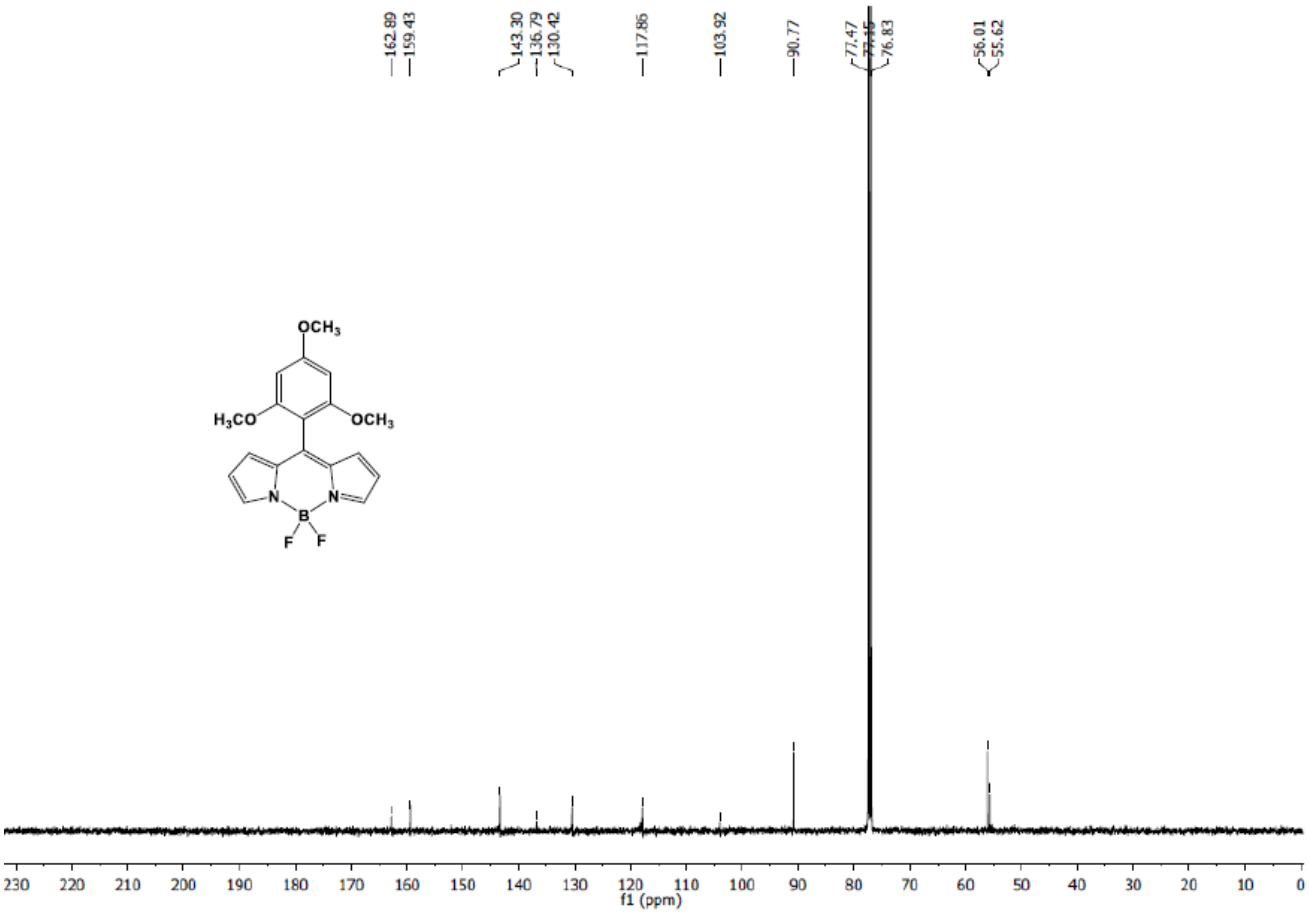

Figure S17. ^{13}C NMR spectrum **BDP-7** (101 MHz, *$CDCl_3$*, 25 °C).

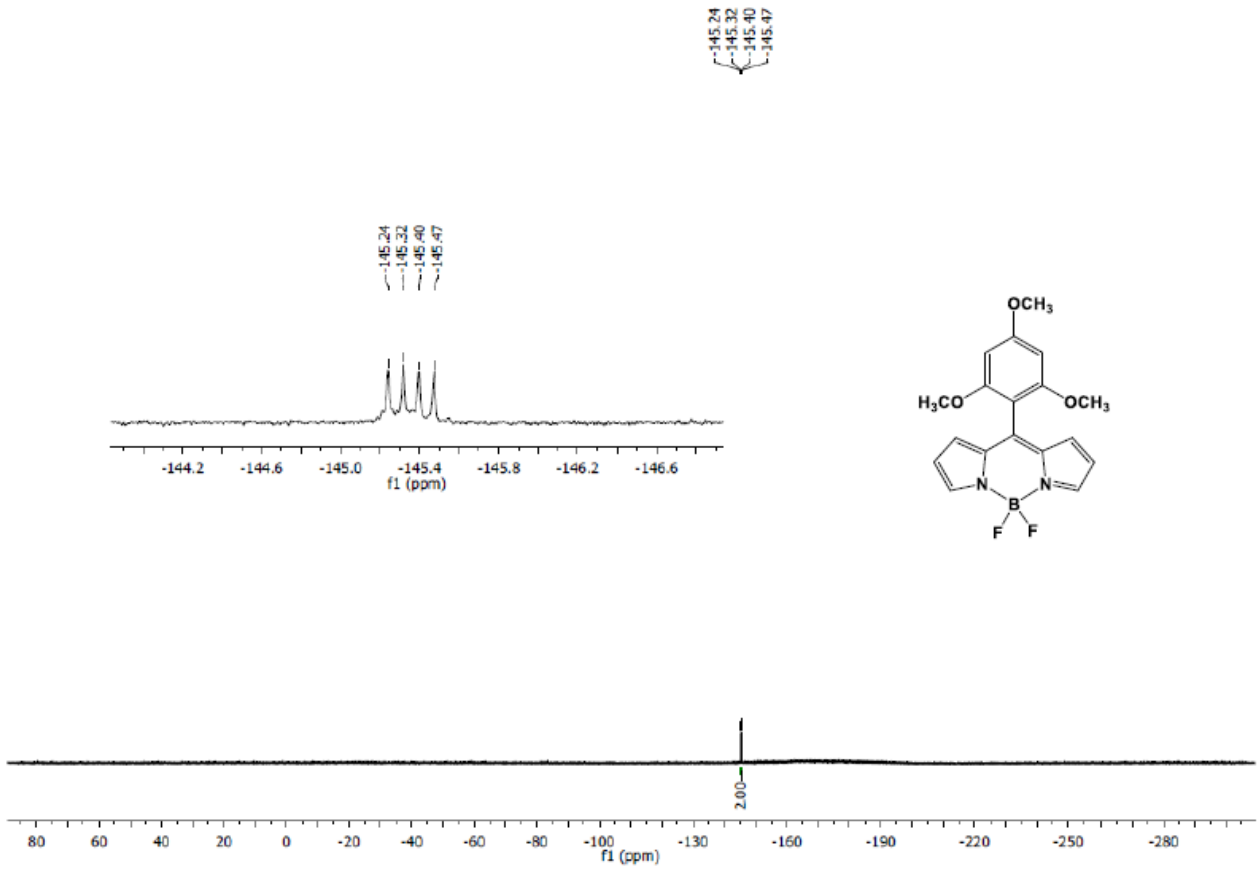

Figure S18. ^{19}F NMR spectrum of **BDP-7** (377 MHz, *$CDCl_3$*, 25 °C).

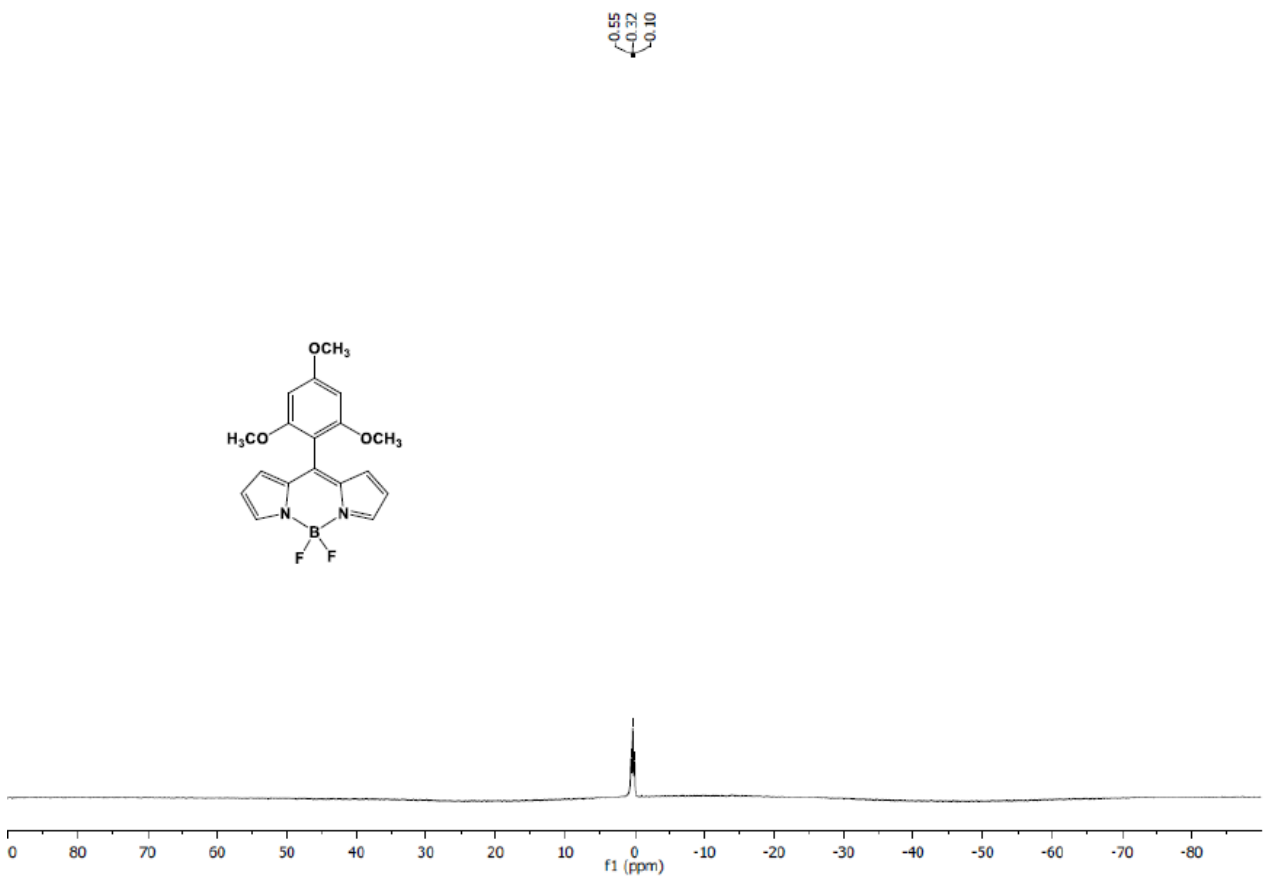

Figure S19. ^{11}B NMR spectrum of **BDP-7** (128 MHz, $CDCl_3$, 25 °C).

Sample-ID		Station	
Submitter		Supervisor	
Analysis Name	AST-2020-14_RB1_01_23763.d	Acquisition Date	30/09/2020 12:09:25
Sample Description			

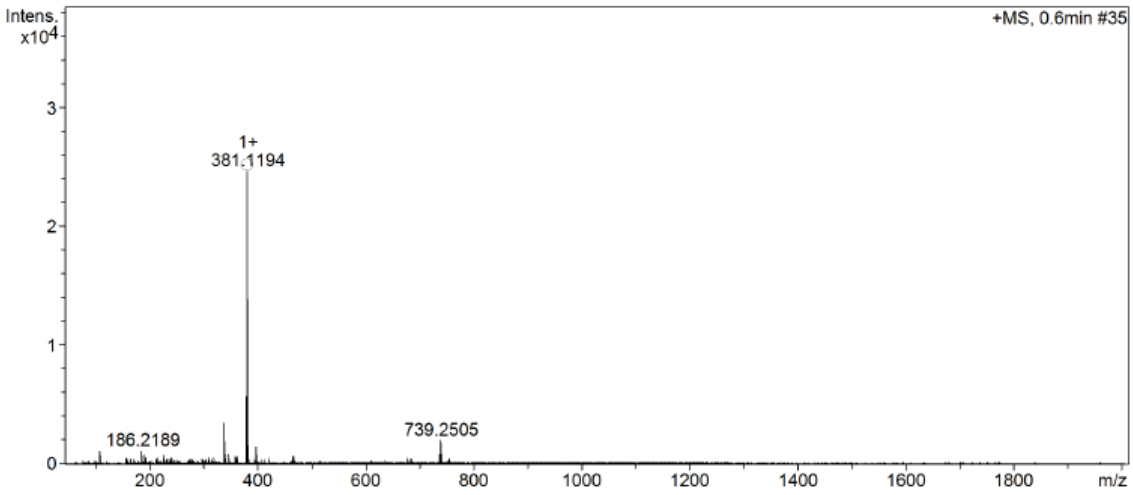

Meas. m/z	#	Ion Formula	m/z	err [mDa]	err [ppm]	rdb	N-Rule	e⁻ Conf	mSigma
381.119449	1	C18H17BF2N2NaO3	381.119579	-0.1	-0.3	10.5	ok	even	5.9

Figure S20. ESI-MS of **BDP 7**.

2.4 Crystallographic Data

A summary of values related to the crystal structure collections is presented in Table S2; Full crystallographic data is available from the Cambridge Crystallographic Data Centre at https://www.ccdc.cam.ac.uk/structures/ under the deposition numbers listed in Table S2.

All non-H atoms were refined with anisotropic thermal parameters; H-atoms were constrained to geometrically idealized positions with isotropic thermal parameters riding on the bound C-atom (HFIX 43 and 137). No special constraints were placed on the molecules presented.

Table S2. Data relating to the crystal structure refinement of compounds **BDP 4-7**.

Identification code	**BDP 4**	**BDP 5**	**BDP 6**	**BDP 7**
Deposition Number (CCDC)	2069560	2069563	2069562	2069561
Chemical formula	$C_{17.5}H_{16}BClF_2N_2O_2$	$C_{17}H_{15}BF_2N_2O_2$	$C_{18}H_{17}BF_2N_2O_3$	$C_{18}H_{17}BF_2N_2O_3$
Formula weight	370.58 g/mol	328.12 g/mol	358.14 g/mol	358.14 g/mol
Crystal size (mm)	0.094 × 0.102 × 0.309	0.112 × 0.301 × 0.734	0.110 × 0.114 × 0.298	0.072 × 0.391 × 0.566
Crystal system	monoclinic	monoclinic	orthorhombic	triclinic
Space group	$P2_1/c$	$P2_1/n$	$P2_12_12_1$	P-1
Unit cell dimensions				
a (Å)	12.5473(4)	10.9508(2)	7.5935(6)	9.4819(8)
b (Å)	20.8955(7)	7.63110(10)	9.4846(8)	9.5287(8)
c (Å)	14.4543(5)	18.1705(3)	23.2455(19)	10.2985(9)
α (°)	90	90	90	63.849(3)
β (°)	115.5179(14)	96.4790(8)	90	84.311(4)
γ (°)	90	90	90	79.654(3)
Volume (Å³)	3420.0(2)	1508.75(4)	1674.2(2)	821.43(12)
Z	8	4	4	2
ρ (calc.) (g/cm³)	1.439	1.445	1.421	1.448
2Θ max. (°)	136.70	90.78	61.02	73.46
Radiation	CuK_α	MoK_α	MoK_α	MoK_α
Wavelength (Å)	1.54178	0.71073	0.71073	0.71073
Scan mode	ω and ϕ	ω and ϕ	ω and ϕ	ω and ϕ
Temperature (K)	100(2)	100(2)	100(2)	100(2)
Reflections collected	28641	139995	63985	53828
Independent reflections	6276	12704	5111	8150
Absorption coefficient (mm^{-1})	2.296	0.111	0.111	0.113
Absorption correction	Multi-Scan	Multi-Scan	Multi-Scan	Multi-Scan
Max. and min. transmission	0.7531 and 0.6219	0.7489 and 0.6689	0.7461 and 0.6228	0.7471 and 0.5839
Structure solution technique	direct methods	direct methods	direct methods	direct methods
Structure solution program	SHELXT 2018/2	SHELXT 2018/2	SHELXT 2018/2	SHELXT 2018/2
Refinement program	SHELXL-2018/3	SHELXL-2018/3	SHELXL-2018/3	SHELXL-2018/3
Data / restraints / parameters	6276 / 0 / 464	12704 / 0 / 219	5111 / 0 / 238	8150 / 0 / 238
H-atom treatment	constr.	constr.	constr.	constr.
R1 (I>2σ(I))	0.0468,	0.0459	0.0455	0.0574
R1 (all data)	0.0522	0.0586	0.0727	0.0925
wR2 (I>2σ(I))	0.1304	0.1165	0.1011	0.1507
wR2 (all data)	0.1353	0.1262	0.1143	0.1776
Goodness-of-fit on F^2	1.067	1.182	1.044	1.037
Refinement Method	Full-matrix least-squares on F^2	Full-matrix least-squares on F^2	Full-matrix least-squares on F^2	Full-matrix least-squares on F^2
Largest diff. peak and hole (eÅ^{-3})	0.904 and -1.102	0.738 and -0.282	0.295 and -0.243	0.696 and -0.464
Flack parameter	-	-	0.2(3)[23]	-

SHELXL-2018/3;[24] SHELXT-2018/2;[25] *refined as a minimisation of $\Sigma\, w(F_o^2 - F_c^2)^2$

2.5 Optical Spectra

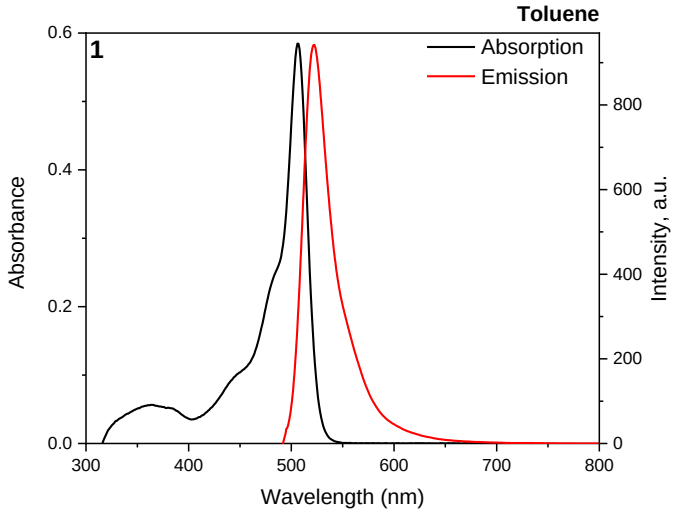

Figure S21. Absorption and emission spectra of **BDP-1**.

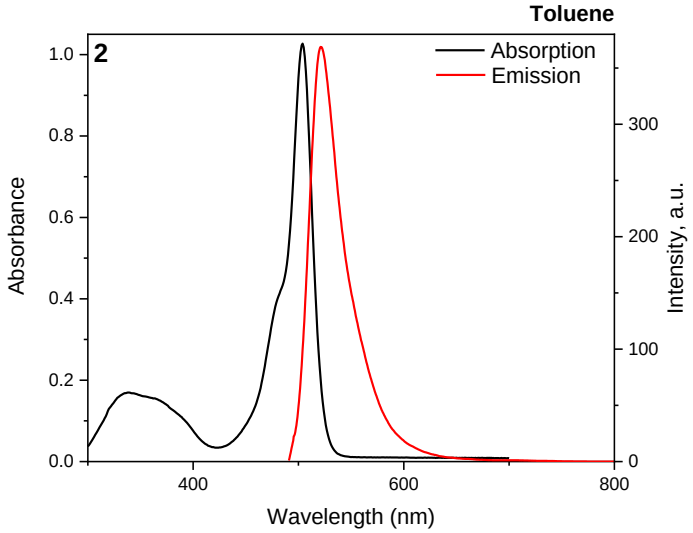

Figure S22. Absorption and emission spectra of **BDP-2**.

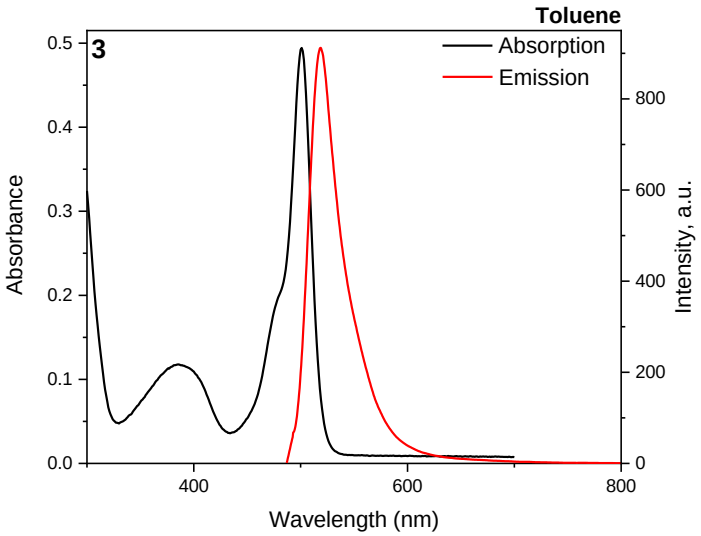

Figure S23. Absorption and emission spectra of **BDP-3**.

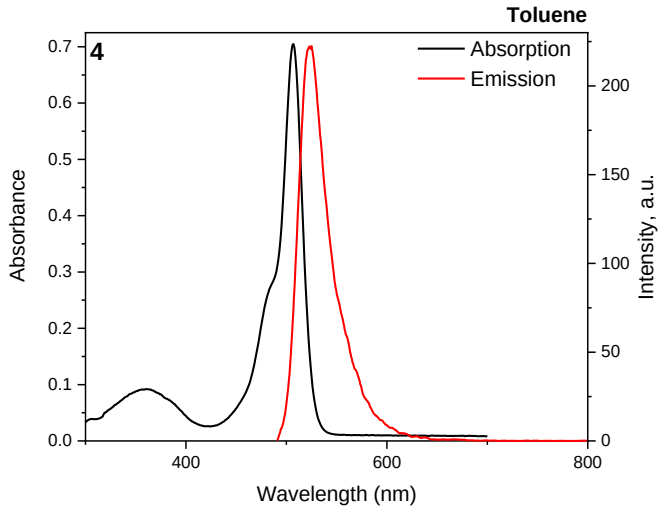

Figure S24. Absorption and emission spectra of **BDP-4**.

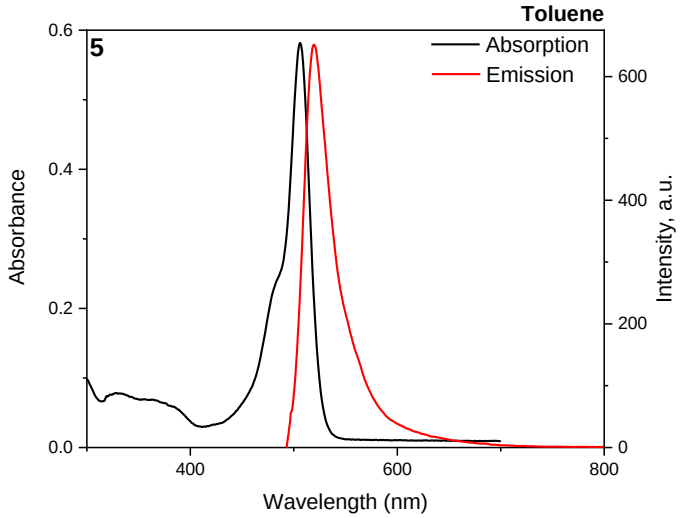

Figure S25. Absorption and emission spectra of **BDP-5**.

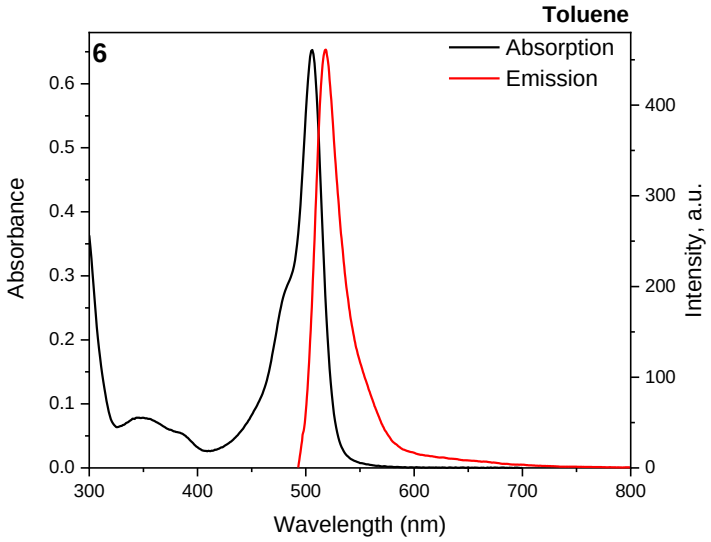

Figure S26. Absorption and emission spectra of **BDP-6**.

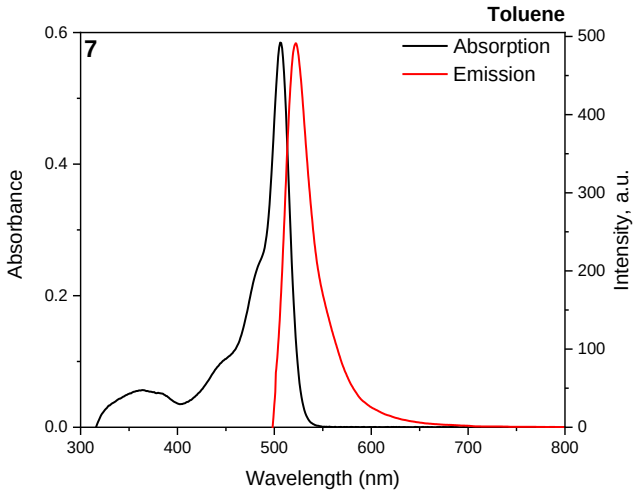

Figure S27. Absorption and emission spectra of **BDP-7**.

3. Computational methods and results

Table S3. Experimental and predicted Log Φ_Δ values of 48 BODIPYs according to Model 1 (toluene).

Compound	Φ_Δ exp. %	Log Φ_Δ exp.	Log Φ_Δ pred.	Residual Log Φ_Δ
3	12	0.785	0.208	0.577
4	6.1	0.362	0.351	0.011
26	2.3	0.633	0.425	0.209
30	4.3	0.820	0.902	-0.082
31 test	6.6	0.580	0.993	-0.413
38	3.8	0.653	0.790	-0.137
40	4.5	1.000	1.060	-0.060
41 test	10	1.301	1.367	-0.066
42	20	1.041	0.986	0.055
48	11	0.934	1.205	-0.271
50	8.6	1.491	0.978	0.513
51	31	1.255	1.387	-0.132
53	18	1.828	1.743	0.085
54	67.3	1.391	1.270	0.121
55 test	24.6	0.903	1.272	-0.368
56	8	0.301	0.372	-0.071
58	2	1.623	1.697	-0.073
59	42	1.362	1.193	0.169
60	23	1.255	1.241	0.014
61	18	1.591	1.130	0.461
62	39	0.602	0.904	-0.302
63 test	4	0.000	0.393	-0.393
64	1	0.146	0.412	-0.266
66	1.4	0.699	0.731	-0.032
67	5	0.519	0.398	0.120
68	3.3	0.362	0.526	-0.164
69	2.3	0.919	1.004	-0.085
70	8.3	0.954	1.161	-0.207
71	9	1.041	0.879	0.162
72 test	11	1.279	1.123	0.156
73	19	1.505	1.539	-0.034
75	32	0.602	0.592	0.010
76	4	1.079	0.899	0.181
77	12	1.602	1.473	0.129
78 test	40	1.602	1.656	-0.054
79	40	1.477	1.676	-0.199
80 test	30	1.477	1.290	0.187
81	30	1.380	1.249	0.131
82 test	24	1.643	1.363	0.280
83	44	1.158	0.990	0.169
84 test	14.4	0.000	0.257	-0.257
BDP-1 ext	1	-0.046	0.513	-0.559
BDP-2 ext	0.9	-0.301	0.169	-0.470
BDP-3	0.5	-0.301	0.146	-0.447
BDP-4	0.5	0.342	0.948	-0.606
BDP-5 ext	2.2	1.400	0.947	0.452
BDP-6	25.1	1.199	1.146	0.052
BDP-7 ext	15.8	1.041	0.959	0.082

Table S4. Experimental and predicted Log Φ_Δ values of 45 BODIPYs according to Model 2 (acetonitrile).

Compound	Φ_Δ exp. %	Log Φ_Δ exp.	Log Φ_Δ pred.	Residual Log Φ_Δ
3 test	6.9	0.839	0.832	0.007
4	1.7	0.230	0.286	-0.056
9 test	2	0.301	0.450	-0.149
10	0.44	-0.357	-0.253	-0.104
11 test	0.43	-0.367	-0.062	-0.304
12 test	0.49	-0.310	-0.784	0.474
13	2.4	0.380	0.175	0.205
14 test	3.7	0.568	0.299	0.269
15	18	1.255	1.048	0.207
16 test	18	1.255	1.500	-0.245
17 test	12.5	1.097	1.030	0.067
18	3.3	0.519	0.715	-0.197
19	31	1.491	1.326	0.165
20	6.2	0.792	1.427	-0.635
21	5.2	0.716	0.532	0.184
22	8.3	0.919	1.085	-0.166
23	5.7	0.756	0.520	0.236
24	8.3	0.919	1.026	-0.107
25	3.3	0.519	0.405	0.114
26	5.7	0.756	1.070	-0.314
27	87.2	1.941	1.414	0.526
28	8.1	0.908	0.454	0.454
29	1.1	0.041	0.377	-0.335
30	8.4	0.924	0.718	0.206
31 test	9.2	0.964	0.992	-0.028
38	22	1.342	1.598	-0.255
40	84	1.924	1.254	0.670
41	11	1.041	1.408	-0.366
42	0.5	-0.301	-0.352	0.051
48	34	1.531	1.446	0.086
51	11	1.041	1.051	-0.010
65	0.9	-0.046	-0.232	0.186
67	2.4	0.380	0.500	-0.120
68	54	1.732	1.370	0.362
74	2.9	0.462	0.807	-0.344
81	25	1.398	1.257	0.141
83	11.2	1.049	1.111	-0.062
84	3	0.477	0.701	-0.224
BDP-1 ext	4.1	0.613	0.263	0.350
BDP-2 ext	0.4	-0.398	-0.241	-0.157
BDP-3	0.7	-0.155	-0.180	0.025
BDP-4	5.9	0.771	0.914	-0.143
BDP-5 ext	0.3	-0.523	0.084	-0.607
BDP-6	0.4	-0.398	-0.017	-0.381
BDP-7 ext	19.3	1.286	0.965	0.321

Table S5. Experimental and predicted Log Φ_Δ values of 41 BODIPYs according to Model 3 (THF).

Compound	Φ_Δ exp. %	Log Φ_Δ exp.	Log Φ_Δ pred.	Residual Log Φ_Δ
1	7.1	0.851	0.533	0.318
3 test	9.1	0.959	0.905	0.054
4	13	1.114	1.000	0.114
9	2.6	0.415	0.382	0.033
10	2.8	0.447	0.468	-0.021
11	1.9	0.279	0.420	-0.141
12	2.6	0.415	-0.079	0.494
13 test	1.2	0.079	0.154	-0.075
14	2.4	0.380	0.704	-0.324
15	6.1	0.785	0.757	0.029
16	5.1	0.708	0.891	-0.183
17	46.2	1.665	0.962	0.702
18	35.7	1.553	1.179	0.373
19	5.9	0.771	0.834	-0.063
20	62.3	1.794	1.672	0.122
21	32.1	1.507	1.547	-0.041
22	61.2	1.787	1.682	0.105
23 test	40.1	1.603	1.580	0.024
24	53.5	1.728	1.750	-0.022
25	33.8	1.529	1.694	-0.165
26	13	1.114	0.912	0.202
27 test	23.2	1.365	1.782	-0.417
28 test	44.2	1.645	1.522	0.124
29	19	1.279	1.505	-0.226
30	15	1.176	1.175	0.001
31 test	6.6	0.820	0.820	-0.001
38	21	1.322	1.103	0.219
48	20	1.301	1.409	-0.108
51	21	1.322	1.353	-0.031
63	0.3	-0.523	-0.551	0.028
64	0.6	-0.222	-0.255	0.034
65 test	0.8	-0.097	-0.495	0.398
66	0.4	-0.398	-0.003	-0.395
81	86	1.934	1.738	0.197
BDP-1 ext	1.1	0.041	0.561	-0.519
BDP-2 ext	0.8	-0.097	0.433	-0.530
BDP-3	2.1	0.322	0.399	-0.077
BDP-4	3.6	0.556	0.847	-0.290
BDP-5 ext	6.1	0.785	0.800	-0.015
BDP-6	1.1	0.041	0.926	-0.885
BDP-7 ext	36.3	1.560	1.139	0.421

4. Singlet oxygen generation quantum yields measurements

The singlet oxygen quantum yield measurements were performed according to the literature.[26] Solutions of the $^1O_2$ trap, 1,9-dimethylanthracene (DMA), with an optical density of around 1.4 in air-saturated solvent (acetonitrile, toluene, and tetrahydrofuran respectively) were employed. Corresponding BODIPY was added to the cuvette, and its absorbance was adjusted to around 0.29 at the wavelength of irradiation. The solutions in the cuvette were irradiated with 514 nm laser light at a constant power density of 12 mW cm^{-2}. The absorption spectra of the solutions were measured every 30 - 90 s. The slope of plots of absorbance of DMA at 376 nm vs. irradiation time for each photosensitizer was calculated.

Singlet oxygen quantum yields were calculated based on the equation:

$$\Phi_\Delta = \Phi_\Delta^{ref} \times \frac{k}{k_{ref}} \times \frac{I_{abs}^{ref}}{I_{abs}}$$

where Φ_Δ is the singlet oxygen quantum yield; the superscript ref stands for 2,6-diiodoBODIPY (0.85 in toluene)[27]; k is the slope of the curves of DMA absorption (376 nm) change vs. irradiation time; I_{abs} represents the absorption correction factor which is given by $I = 1–10^{-OD}$ (OD is the optical density at 514 nm).

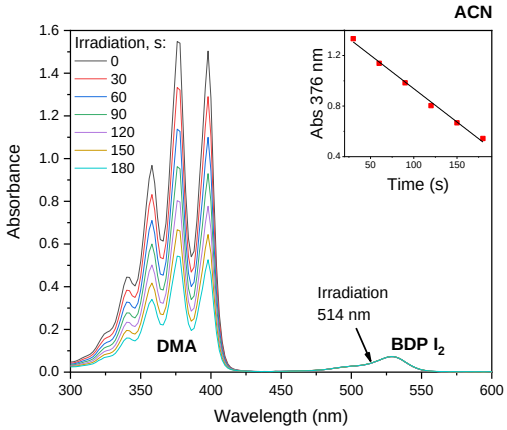

Figure S28. Photooxidation of 1,9-dimethylanthracene in air-saturated acetonitrile solution containing reference photosensitizer - 2,6-diiodoBODIPY. Inset: dependence of absorbance at 376 nm on the irradiation time.

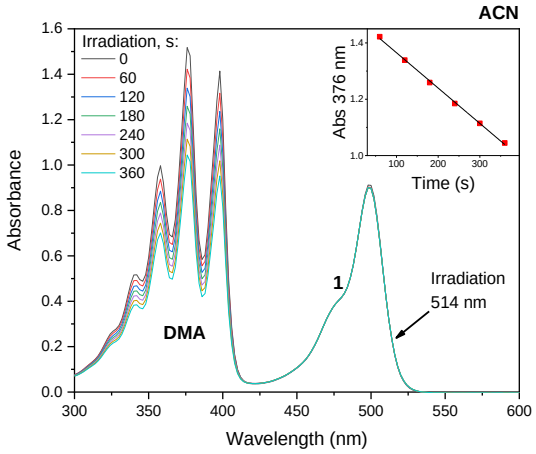

Figure S29. Photooxidation of 1,9-dimethylanthracene in air-saturated acetonitrile solution containing **BDP-1**. Inset: dependence of absorbance at 376 nm on the irradiation time.

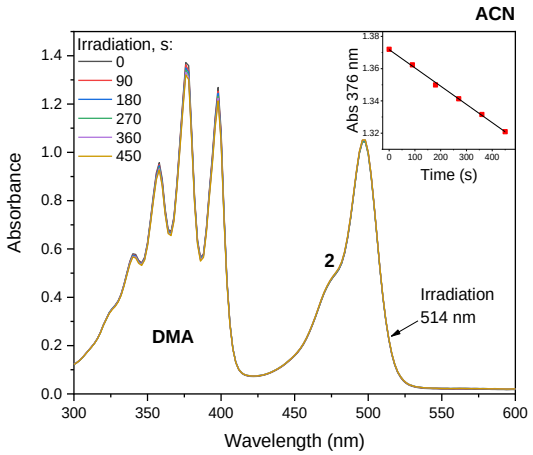

Figure S30. Photooxidation of 1,9-dimethylanthracene in air-saturated acetonitrile solution containing **BDP-2**. Inset: dependence of absorbance at 376 nm on the irradiation time.

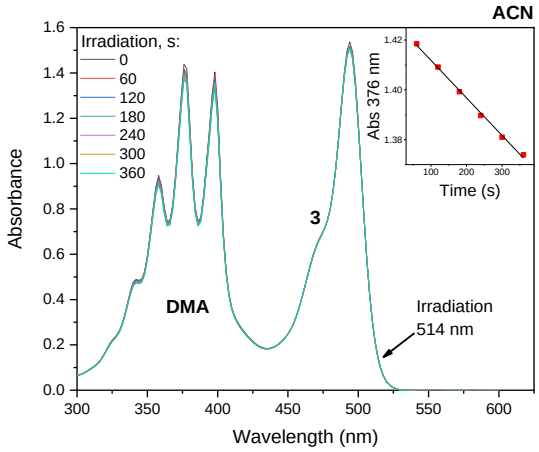

Figure S31. Photooxidation of 1,9-dimethylanthracene in air-saturated acetonitrile solution containing **BDP-3**. Inset: dependence of absorbance at 376 nm on the irradiation time.

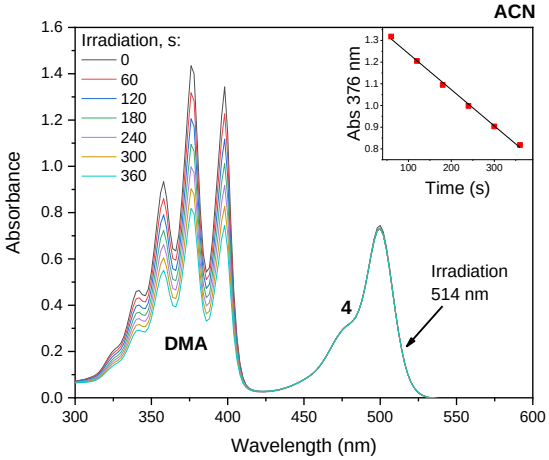

Figure S32. Photooxidation of 1,9-dimethylanthracene in air-saturated acetonitrile solution containing **BDP-4**. Inset: dependence of absorbance at 376 nm on the irradiation time.

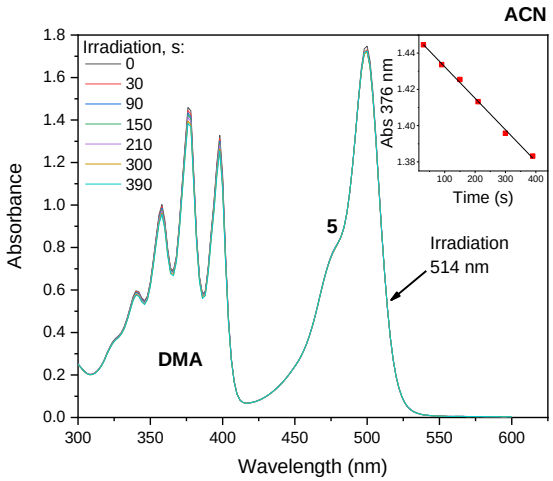

Figure S33. Photooxidation of 1,9-dimethylanthracene in air-saturated acetonitrile solution containing **BDP-5**. Inset: dependence of absorbance at 376 nm on the irradiation time.

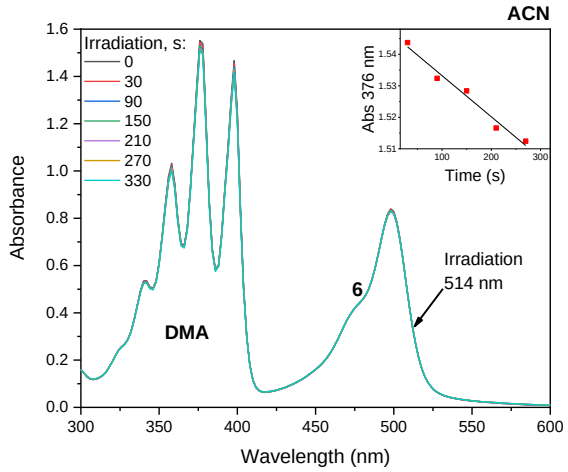

Figure S34. Photooxidation of 1,9-dimethylanthracene in air-saturated acetonitrile solution containing **BDP-6**. Inset: dependence of absorbance at 376 nm on the irradiation time.

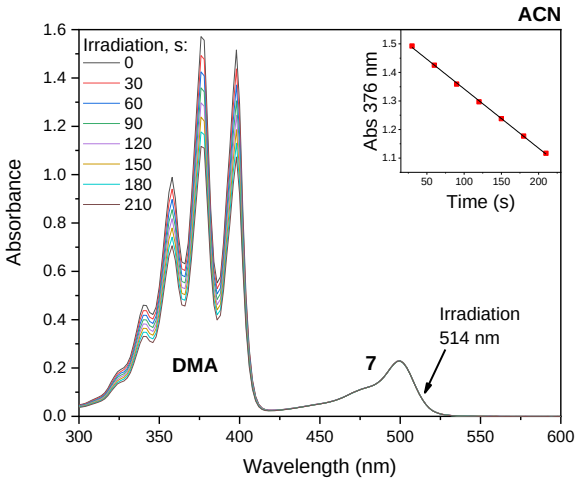

Figure S35. Photooxidation of 1,9-dimethylanthracene in air-saturated acetonitrile solution containing **BDP-7**. Inset: dependence of absorbance at 376 nm on the irradiation time.

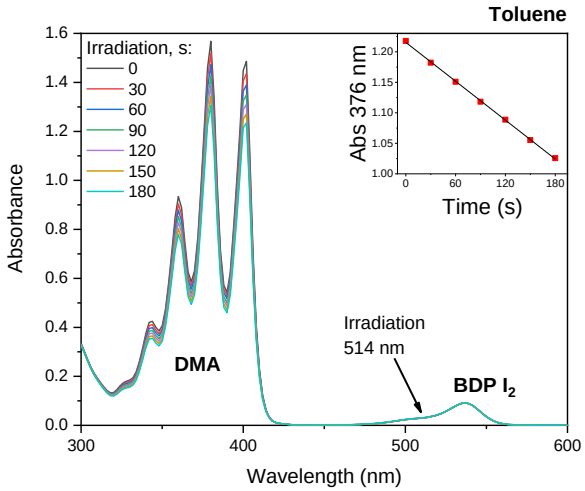

Figure S36. Photooxidation of 1,9-dimethylanthracene in air-saturated toluene solution containing reference photosensitizer - 2,6-diiodoBODIPY. Inset: dependence of absorbance at 376 nm on the irradiation time.

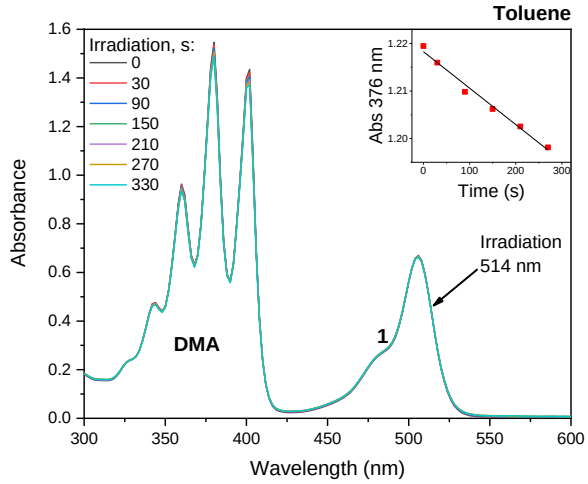

Figure S37. Photooxidation of 1,9-dimethylanthracene in air-saturated toluene solution containing **BDP-1**. Inset: dependence of absorbance at 376 nm on the irradiation time.

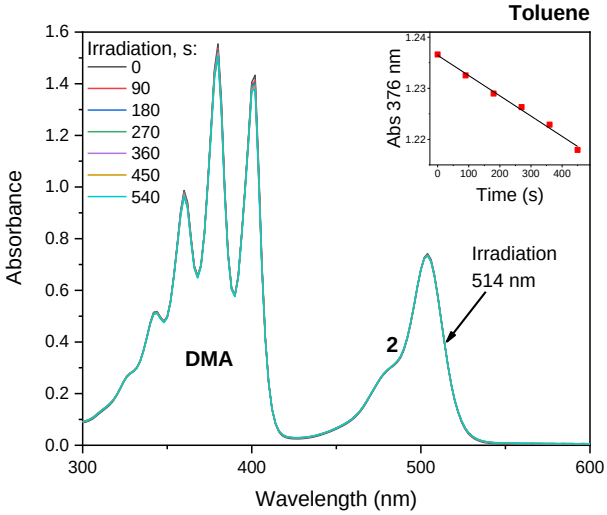

Figure S38. Photooxidation of 1,9-dimethylanthracene in air-saturated toluene solution containing **BDP-2**. Inset: dependence of absorbance at 376 nm on the irradiation time.

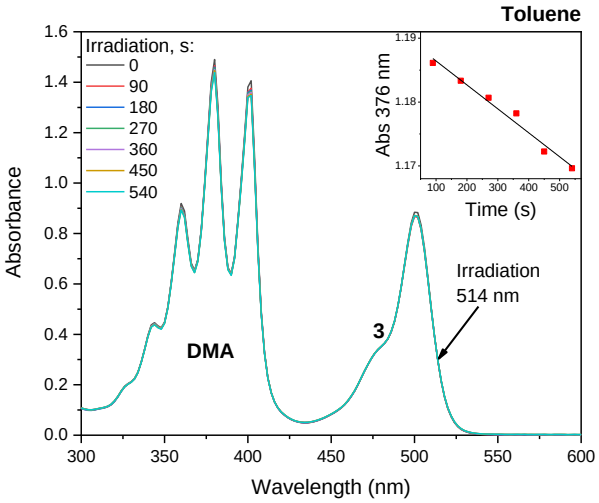

Figure S39. Photooxidation of 1,9-dimethylanthracene in air-saturated toluene solution containing **BDP-3**. Inset: dependence of absorbance at 376 nm on the irradiation time.

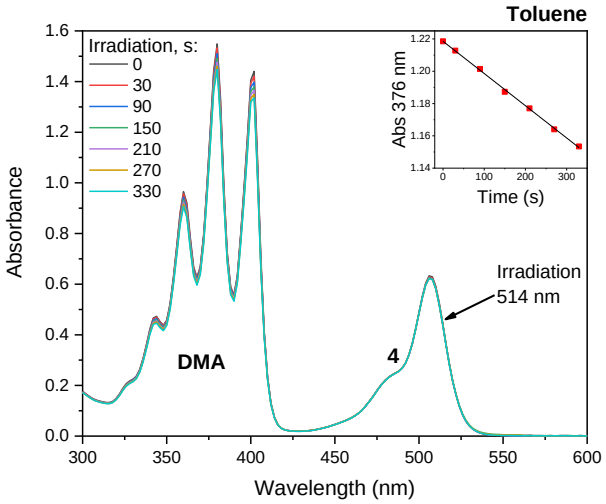

Figure S40. Photooxidation of 1,9-dimethylanthracene in air-saturated toluene solution containing **BDP-4**. Inset: dependence of absorbance at 376 nm on the irradiation time.

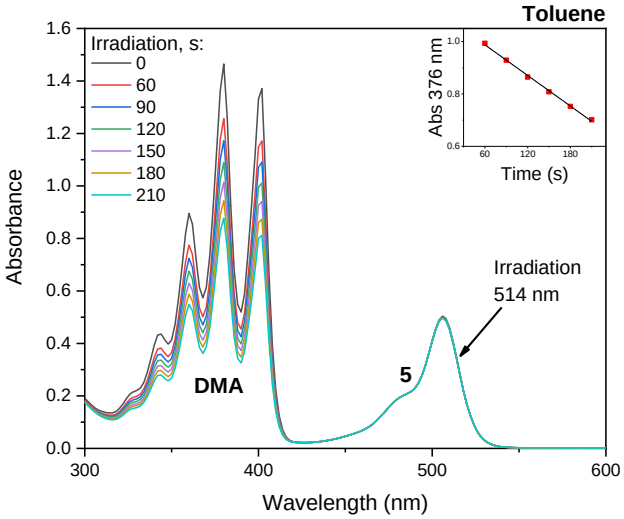

Figure S41. Photooxidation of 1,9-dimethylanthracene in air-saturated toluene solution containing **BDP-5**. Inset: dependence of absorbance at 376 nm on the irradiation time.

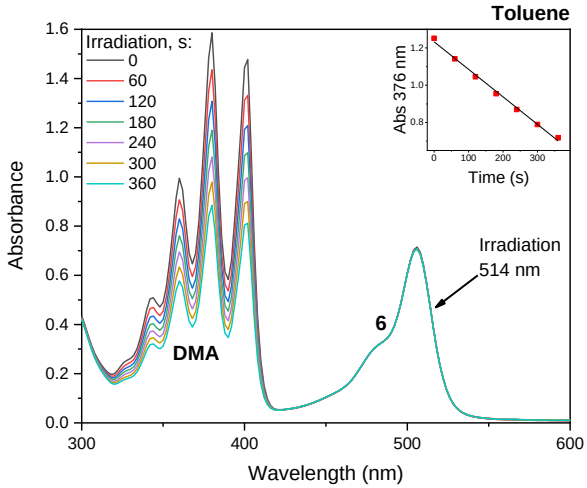

Figure S42. Photooxidation of 1,9-dimethylanthracene in air-saturated toluene solution containing **BDP-6**. Inset: dependence of absorbance at 376 nm on the irradiation time.

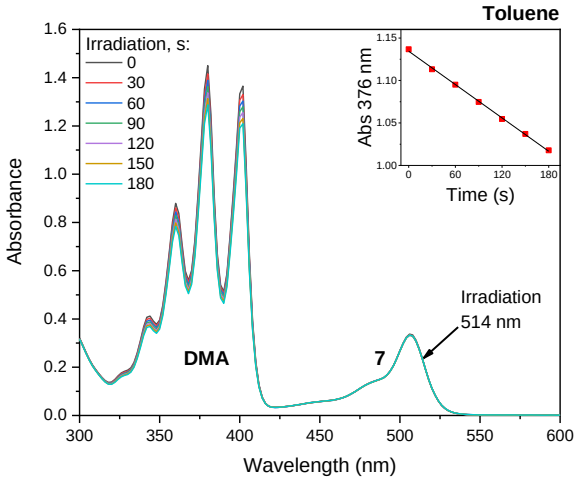

Figure S43. Photooxidation of 1,9-dimethylanthracene in air-saturated toluene solution containing **BDP-7**. Inset: dependence of absorbance at 376 nm on the irradiation time.

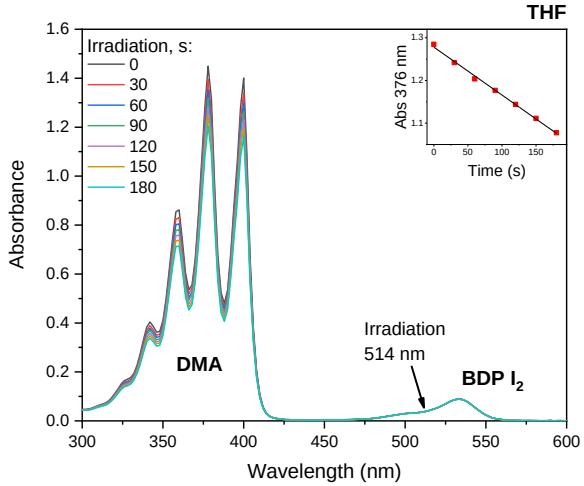

Figure S44. Photooxidation of 1,9-dimethylanthracene in air-saturated THF solution containing reference photosensitizer - 2,6-diiodoBODIPY. Inset: dependence of absorbance at 376 nm on the irradiation time.

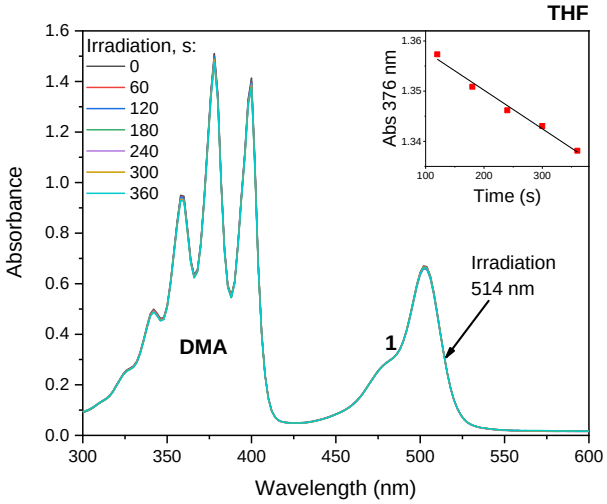

Figure S45. Photooxidation of 1,9-dimethylanthracene in air-saturated THF solution containing **BDP-1**. Inset: dependence of absorbance at 376 nm on the irradiation time.

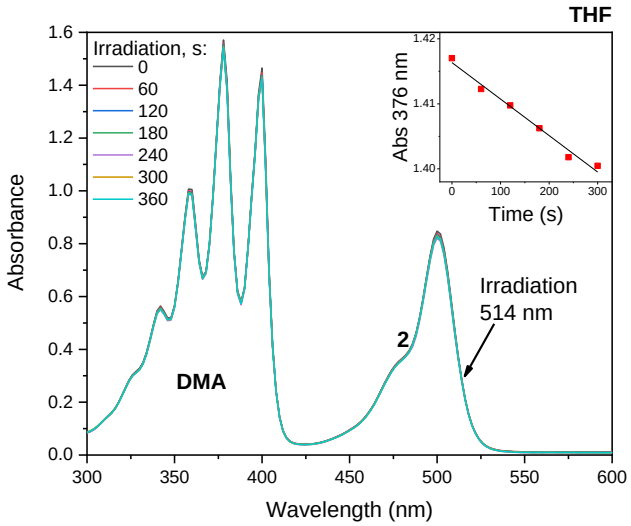

Figure S46. Photooxidation of 1,9-dimethylanthracene in air-saturated THF solution containing **BDP-2**. Inset: dependence of absorbance at 376 nm on the irradiation time.

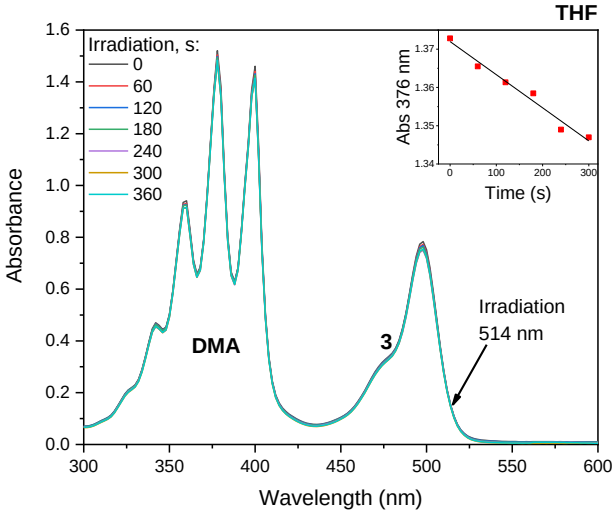

Figure S47. Photooxidation of 1,9-dimethylanthracene in air-saturated THF solution containing **BDP-3**. Inset: dependence of absorbance at 376 nm on the irradiation time.

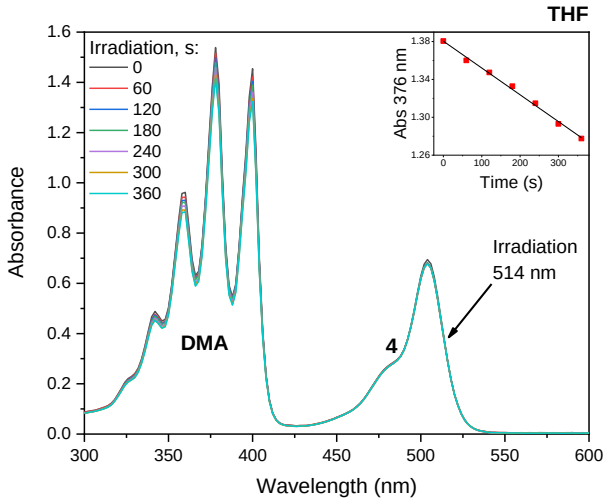

Figure S48. Photooxidation of 1,9-dimethylanthracene in air-saturated THF solution containing **BDP-4**. Inset: dependence of absorbance at 376 nm on the irradiation time.

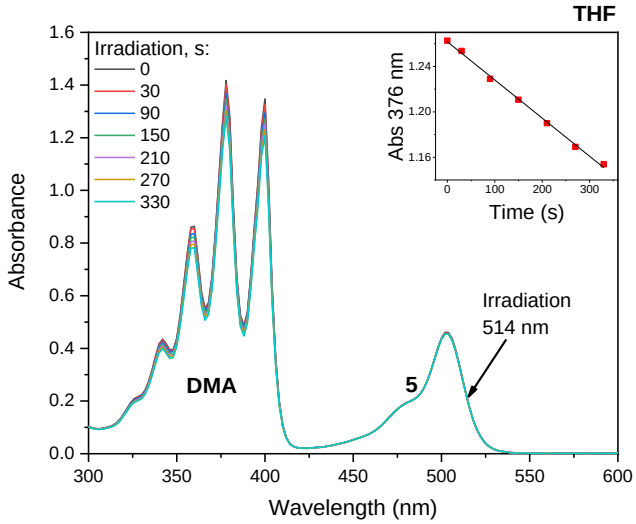

Figure S49. Photooxidation of 1,9-dimethylanthracene in air-saturated THF solution containing **BDP-5**. Inset: dependence of absorbance at 376 nm on the irradiation time.

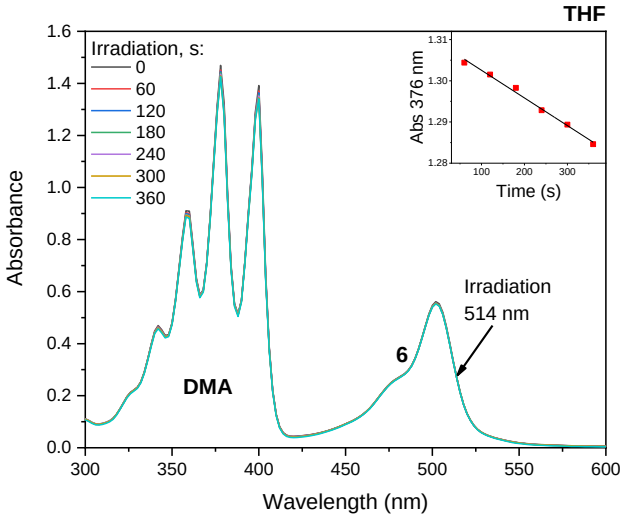

Figure S50. Photooxidation of 1,9-dimethylanthracene in air-saturated THF solution containing **BDP-6**. Inset: dependence of absorbance at 376 nm on the irradiation time.

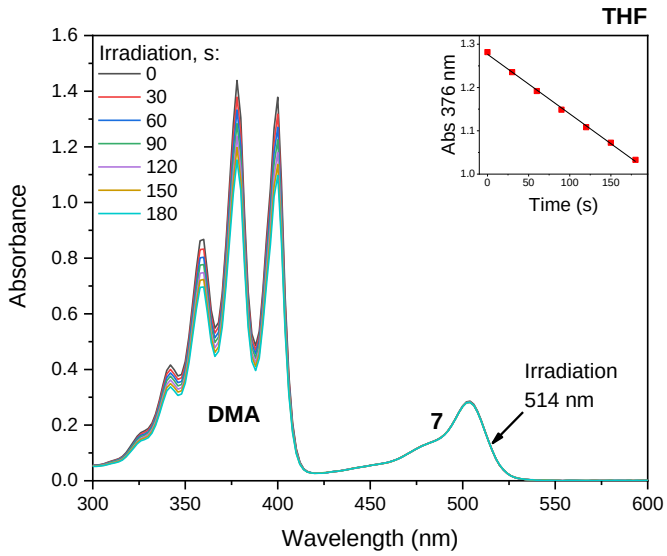

Figure S51. Photooxidation of 1,9-dimethylanthracene in air-saturated THF solution containing **BDP-7**. Inset: dependence of absorbance at 376 nm on the irradiation time.

5. Supplemental Crystal Structure Images

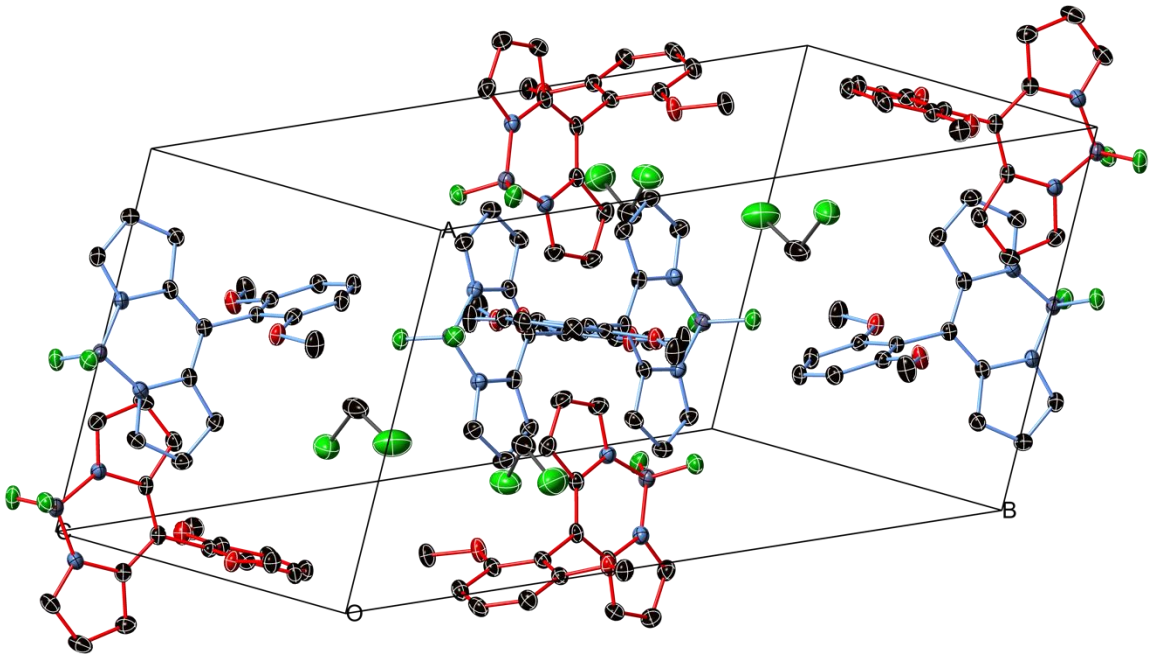

Figure S52. View of the crystallographic unit cell of **BDP-4·½(DCM)**, with the two inequivalent molecules (containing C1 and C101) shown in blue and red bonds, respectively; Thermal ellipsoids are shown at the 50% probability level, H-atoms omitted from view.

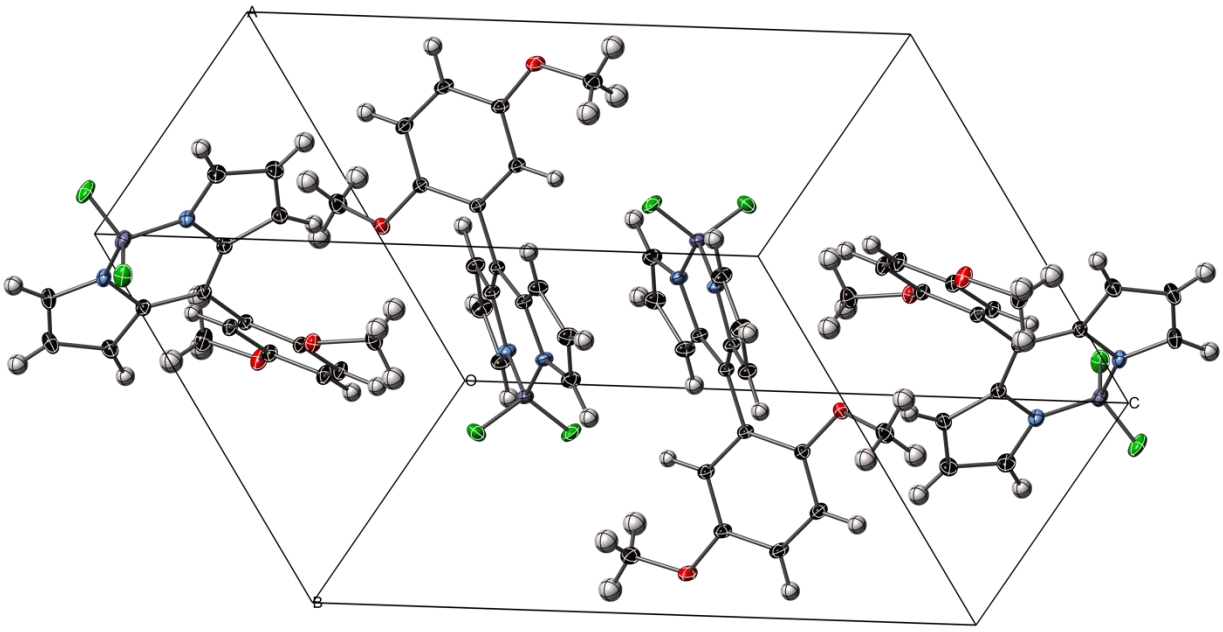

Figure S53. View of the crystallographic unit cell of **BDP-5**; Thermal ellipsoids are shown at the 50% probability level.

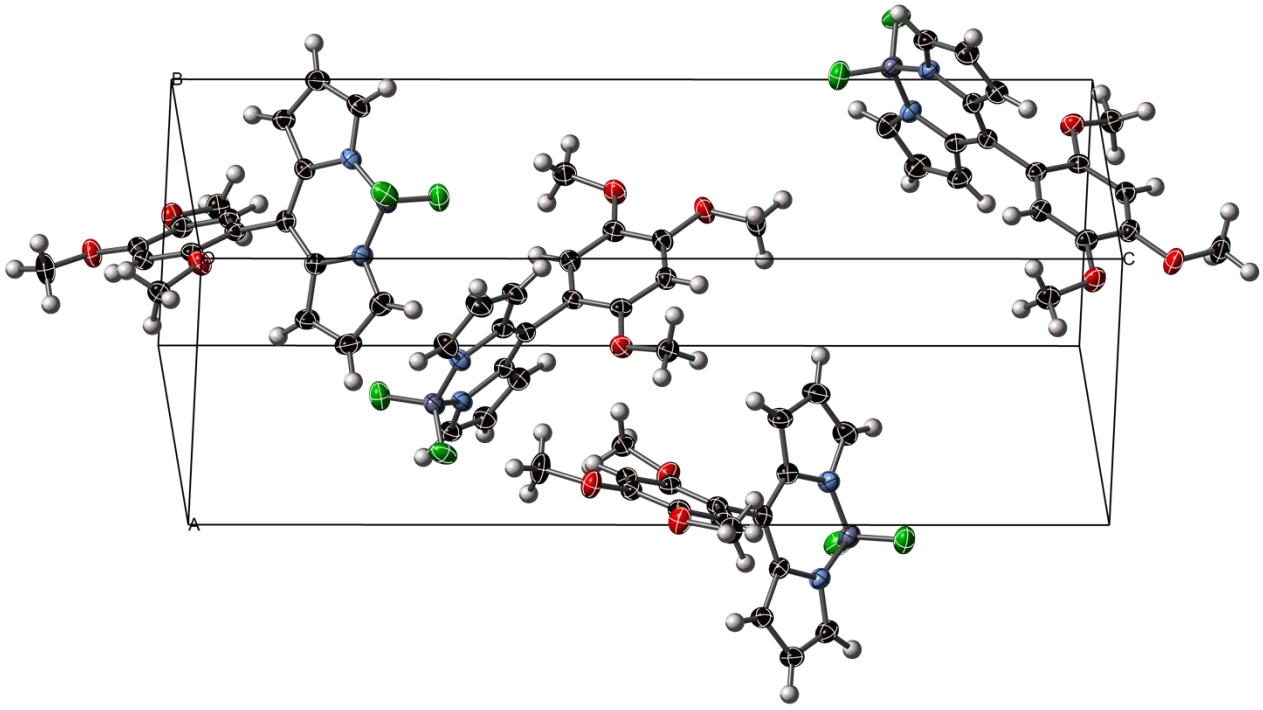

Figure S54. View of the crystallographic unit cell of BDP-6; Thermal ellipsoids are shown at the 50% probability level, H-atoms are represented as spheres of fixed radius.

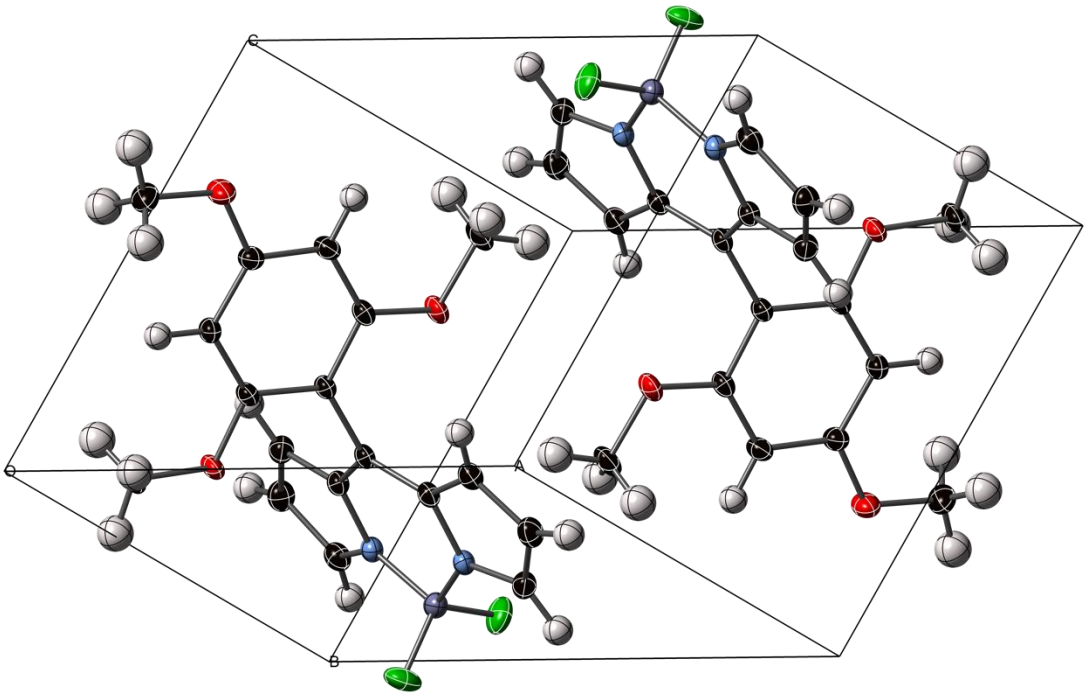

Figure S55. View of the crystallographic unit cell of BDP-7; Thermal ellipsoids are shown at the 50% probability level.

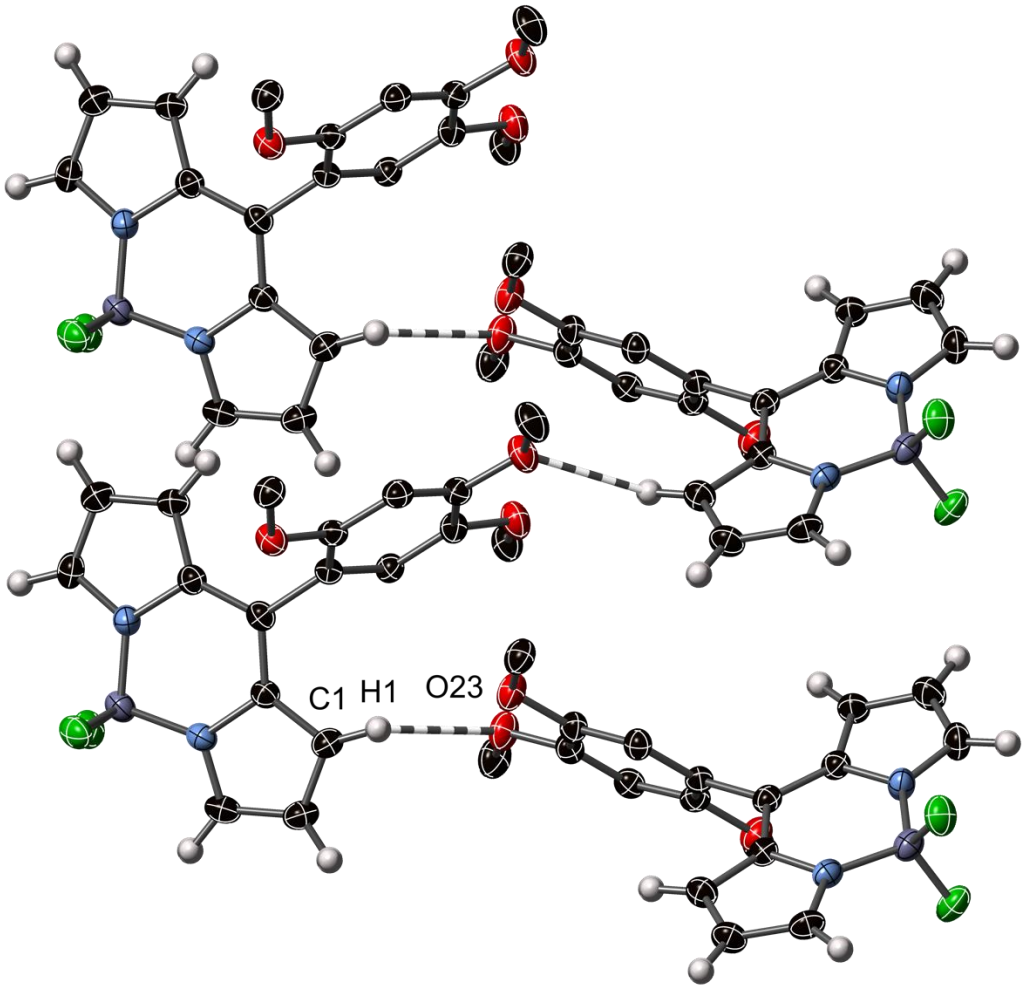

Figure S56. Intermolecular C-H···O interactions in the crystal structure of BDP-6, at 3.28 Å C···O; Thermal ellipsoids are shown at the 50% probability level, H-atoms are represented as spheres of fixed radius.

6. References

[1] X.-F. Zhang, J. Zhu, *J. Luminescence*, 2019, **205**, 148.
[2] X.-F. Zhang, N. Feng, *Spectrochim. Acta A*, 2018, **189**, 13.
[3] W. Hu, M. Liu, X.-F. Zhang, Y. Wang, Y. Wang, H. Lan, H. Zhao, *J. Phys. Chem. C*, 2019, **123**, 15944.
[4] X.-F. Zhang, N. Feng, *Chem. Asian. J.*, 2017, **12**, 2447.
[5] W. Hu, Y. Lin, X.-F. Zhang, M. Feng, S. Zhao, J. Zhang, *Dyes Pigm.*, 2019, **164**, 139.
[6] W. Hu, X.-F. Zhang, X. Lu, S. Lan, D. Tian, T. Li, L. Wang, S. Zhao, M. Feng, J. Zhang, *J. Lumin.*, 2018, **194**, 185.
[7] W. Hua, X.-F. Zhang, X. Lu, S. Lan, D. Tian, T. Li, L. Wang, S. Zhao, M. Feng, J. Zhang, *Dyes Pigm.*, 2018, **149**, 306.
[8] M.A. Filatov, S. Karuthedath, P.M. Polestshuk, S. Callaghan, K.J. Flanagan, M. Telitchko, T. Wiesner, F. Laquai, M.O. Senge, *Phys. Chem. Chem. Phys.*, 2018, **20**, 8016.
[9] Z. Wang, J. Zhao, *Org. Lett.*, 2017, **19**, 4492.
[10] M.A. Filatov, S. Karuthedath, P.M. Polestshuk, S. Callaghan, K. Flanagan, T. Wiesner, F. Laquai, M.O. Senge, *ChemPhotoChem*, 2018, **2**, 606.
[11] Z. Wang, M. Ivanov, Y. Gao, L. Bussotti, P. Foggi, H. Zhang, N. Russo, B. Dick, J. Zhao, M. Di Donato, G. Mazzone, L. Luo, M. Fedin, *Chem. Eur. J.*, 2020, **26**, 1091.
[12] Z. Wang, J. Zhao, M. Di Donato, G. Mazzone, *Chem. Commun.*, 2019, **55**, 1510.
[13] K. Chen, W. Yang, Z. Wang, A. Iagatti, L. Bussotti, P. Foggi, W. Ji, J. Zhao, M. Di Donato, *J. Phys. Chem. A*, 2017, **121**, 7550.
[14] Y. Dong, A.A. Sukhanov, J. Zhao, A. Elmali, X. Li, B. Dick, A. Karatay, V.K. Voronkova, *J. Phys. Chem. C*, 2019, **123**, 22793.
[15] Y. Dong, A. Elmali, J. Zhao, B. Dick, A. Karatay, *ChemPhysChem*, 2020, **21**, 1388.
[16] K. Chen, M. Taddei, L. Bussotti, P. Foggi, J. Zhao, M. Di Donato, *ChemPhotoChem*, 2020, **4**, 487.
[17] Y. Hou, I. Kurganskii, A. Elmali, H. Zhang, Y. Gao, L. Lv, J. Zhao, A. Karatay, L. Luo, M. Fedin, *J. Chem. Phys.*, 2020, **152**, 114701.
[18] V.-N. Nguyen, Y. Yim, S. Kim, B. Ryu, K. M. K. Swamy, G. Kim, N. Kwon, C.-Y. Kim, S. Park, J. Yoon, *Angew. Chem. Int. Ed.*, 2020, **59**, 8957.
[19] B. Ventura, G. Marconi, M. Bröring, R. Krüger, L. Flamigni, *New J. Chem.*, 2009, **33**, 428.
[20] L. Ya, J. Zhao, A. Iagatti, L. Bussotti, P. Foggi, E. Castellucci, M. Di Donato, K. Han, *J. Phys. Chem. C*, 2018, **122**, 2502.
[21] N. Epelde-Elezcano, E. Palao, H. Manzano, A. Prieto-CastaCeda, A.R. Agarrabeitia, A. Tabero, A. Villanueva, S. de la Moya, C. Ljpez-Arbeloa, V. Martinez-Martinez, M.J. Ortiz, *Chem. Eur. J.*, 2017, **23**, 4837
[22] M. Taniguchi and J. S. Lindsey, *Photochem. Photobiol.*, 2018, **94**, 290.
[23] S. Parsons, H. D. Flack, T. Wagner, *Acta Cryst.*, **2013**, B*69*, 249.
24 G. M. Sheldrick, *Acta Cryst.*, **2015**, C*71*, 3.
[25] G. M. Sheldrick, *Acta Cryst.*, **2015**, A*71*, 3.
[26] L. Gou, C. N. Coretsopoulos and A. B. Scranton, *J. Polym. Sci. Part A Polym. Chem.*, 2004, **42**, 1285.
[27] Y. Zhao, R. Duan, J. Zhao and C. Li, *Chem. Commun.*, 2018, **54**, 12329.